Design and synthesis of tripeptidyl furylketones as selective inhibitors against the β5 subunit of human 20S proteasome

Qi Sun, Tongliang Zhou, Dandan Xi, Xiaona Li, Zirui Lü, Fengrong Xu, Chao Wang, Yan Niu, Ping Xu

PII: S0223-5234(20)30127-6

DOI: https://doi.org/10.1016/j.ejmech.2020.112160

Reference: EJMECH 112160

To appear in: *European Journal of Medicinal Chemistry*

Received Date: 29 November 2019

Revised Date: 18 February 2020

Accepted Date: 18 February 2020

Please cite this article as: Q. Sun, T. Zhou, D. Xi, X. Li, Z. Lü, F. Xu, C. Wang, Y. Niu, P. Xu, Design and synthesis of tripeptidyl furylketones as selective inhibitors against the β5 subunit of human 20S proteasome, *European Journal of Medicinal Chemistry* (2020), doi: https://doi.org/10.1016/j.ejmech.2020.112160.

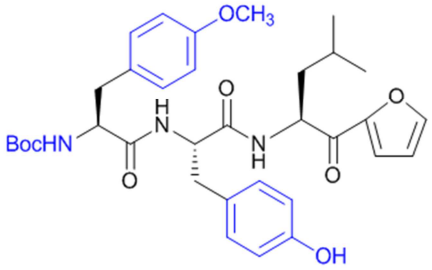

10b'

CT-L: IC_{50} = 1.64 μM
Hela: IC_{50} = 7.03 μM
A375: IC_{50} = 5.66 μM

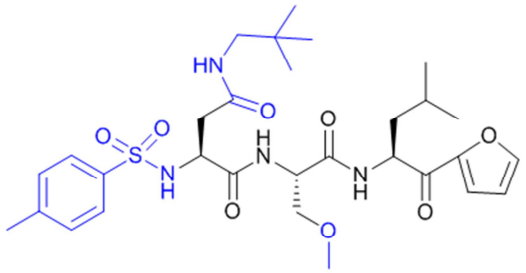

11m

CT-L: IC_{50} = 0.18 μM
Hela: IC_{50} = 0.67 μM
A375: IC_{50} = 0.88 μM
PK data: Cmax, 2007 μg/L; AUC_{0-t}, 680 μg/L·h; Vss, 0.66 L/kg

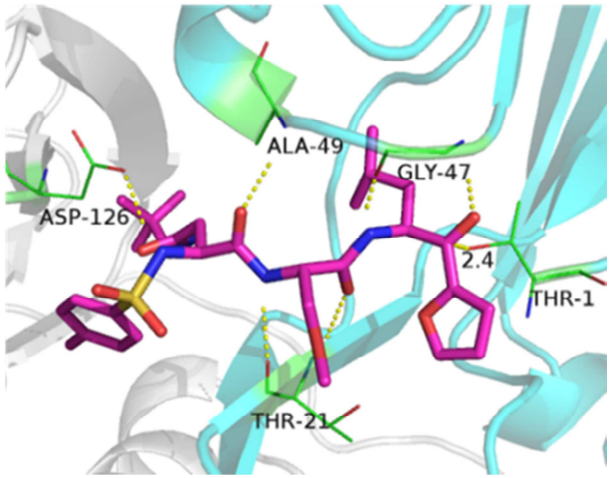

Design and synthesis of tripeptidyl furylketones as selective inhibitors against the β5 subunit of human 20S proteasome

Qi Sun[‡,§], Tongliang Zhou[‡], Dandan Xi, Xiaona Li, Zirui Lü, Fengrong xu, Chao Wang, Yan Niu* and Ping Xu*

Department of Medicinal Chemistry, School of Pharmaceutical Sciences, Peking University Health Science Center, Beijing 100191, China

[‡] These authors contributed equally to this work.

§ The present address can be found at the end of this paper.

*Corresponding authors: yanniu@bjmu.edu.cn (Y. Niu), pingxu@bjmu.edu.cn (P. Xu)

Abstract

A series of tripeptidic proteasome inhibitors with furylketone as C-terminus were designed and synthesized. Biochemical evaluations against β1, β2 and β5 subunits revealed that they acted selectively on β5 subunit with IC_{50}s against chymotrypsin-like (CT-L) activity in micromolar range. LC-MS/MS analysis of the ligand-20S proteasome mixture showed that the most potent compound **11m** (IC_{50} = 0.18 μM) made no covalent modification on 20S proteasome. However, it was identified acting in a slowly reversible manner in wash-out assay and the reversibility was much lower than that of MG132, suggesting the possibility of these tripeptidic furylketones forming reversible covalent bonds with 20S proteasome. Several compounds were selected for anti-proliferative assay towards multiple cancer cell lines, and compound **11m** displayed comparable potency to positive control (MG132) in all cell lines tested. Furthermore, the pharmacokinetic (PK) data in rats indicated **11m** behaved similarly (C_{max}, 2007 μg/L; AUC_{0-t}, 680 μg/L·h; V_{ss}, 0.66 L/kg) to the clinical used agent carfilzomib. All these data suggest **11m** is a good lead compound to be developed to novel anti-tumor agent.

Keywords: Proteasome inhibitors, Peptidic, Furylketone, Anti-tumor

1. Introduction

In eukaryotic cells, the amount of each intracellular protein depends on the balance of its rates of synthesis and degradation. This homeostasis is maintained by two proteolysis systems, namely the ubiquitin-proteasome system (UPS) and the lysosomal degradation pathway [1]. The UPS is responsible for the specific degradation of short-lived regulatory proteins and the removal of damaged soluble proteins, and thus tightly controls a broad array of basic cellular processes including gene transcription, signal transduction, DNA repair, cell cycle regulation, apoptosis, and immune response [2]. The catalytic degradation of polyubiquitinated substrates in the ubiquitin-proteasome pathway (UPP) is performed by 26S proteasome which is a barrel-shaped, multi-catalytic protease complex consisting of a 20S core particle (CP) and two 19S regulatory caps [3]. The 20S CP of the proteasome comprises 28 protein subunits assembled into four heptameric rings: two outer α-rings (α1-α7) and two inner β-rings (β1-β7) [4,5]. The outer α subunits are proteolytically inactive and serve a regulatory function, while the two inner rings each possess three catalytic active β subunits [6-8]. Each of the active β subunits is responsible for a single type of proteolytic activity: β1 for caspase-like (C-L), β2 for trypsin-like (T-L), and β5 for chymotrypsin-like (CT-L) activity. Site-directed mutagenesis analysis of the yeast proteasome has revealed that CT-L activity of proteasome had the greatest impact on proteolysis [9], and inhibition of tumor cellular CT-L activity is a strong stimulus that induces apoptosis [10-12]. These observations have promoted development of numerous synthetic inhibitors of the β5 subunit [13], among which bortezomib, carfilzomib and ixazomib (**Fig. 1A**) have been successfully approved by the US Food and Drug Administration (FDA) in the year of 2003, 2012, and 2015, respectively, for the treatment of multiple myeloma [14].

Recently, we have reported a series of C-terminal furylketone-based peptidic inhibitors against β5 subunit proposing that the C-terminal furylketone could serve as a warhead that form covalent bond with the catalytically active residue, namely Thr1, of the β5 subunit and therefore, could produce high affinity and inhibitory potency. However, only moderate potency was observed on the most potent compound **10b' (Fig. 1B)** with IC_{50} of 1.64 ± 0.44 μM in enzymatic assay [15]. Docking and dynamic simulations suggested that the distance between the C-terminal furylketone of **10b'** and the -OH of residue Thr1 was too large (4.9 Å) to form covalent bond due to the torsional strain brought about from the P^2 and P^3 substitutions. To further explore our hypothesis regarding binding mode, more active compounds are required. In the present study, we extended substitutions on the peptidic backbone at R^2 to R^4 (**Fig. 1C**) aiming at optimized

fitting into the S^2 to S^4 sub-pockets of β5 subunit and therefore, enhanced potency could be achieved as was expected for covalent inhibitors [16]. The binding mode was also discussed based on computational simulations together with wash-out assay and LC-MS/MS analysis.

Selected compounds were evaluated for anti-proliferating effect against a panel of cancer cell lines using MG132 (**Fig. 1D**) as positive control, meanwhile, their cytotoxicities were also measured in nonmalignant cells (HEK293).

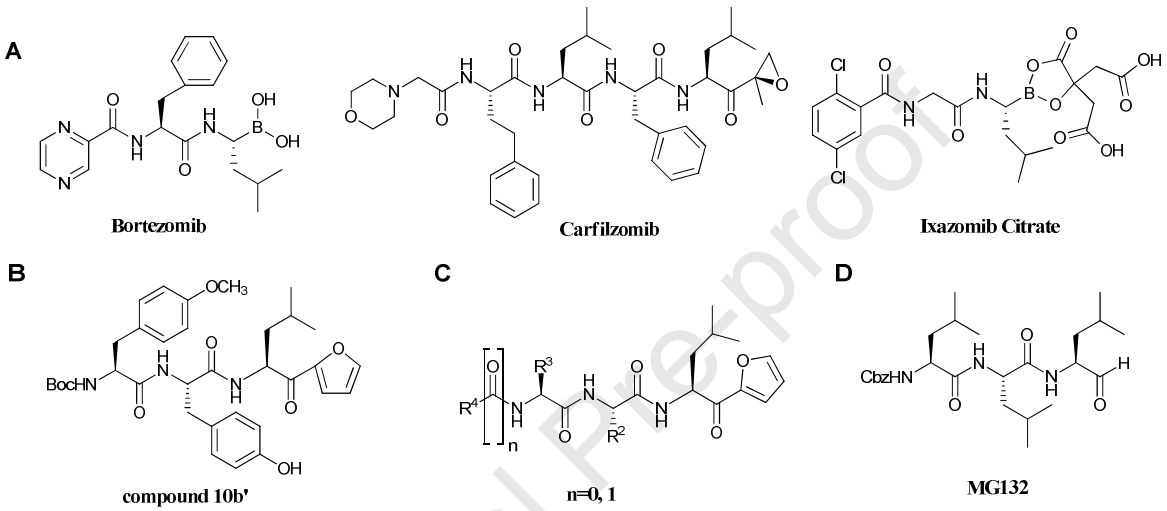

Figure 1. The structures of (A) bortezomib, carfilzomib and ixazomib cirtate; (B) Compound **10b'**, (C) designed tripeptidic inhibitors, (D) MG132.

2. Results and Discussion

2.1 Chemistry.

The design of substitutions at R^2 to R^4 (**Fig. 1C**) on the tripeptidic scaffold was performed according to the structure-activity relationship (SAR) studies on our previously described tripeptidyl furylketones [15,17]. Overall, the best fit into the S2-S4 sub-pockets were explored.

The designed furylketone-based tripeptides (**7a-7j**, **11a-11o**) were acquired through two different synthetic routes. Initially, the furan-based leucine **3** was synthesized starting from commercially available Boc-protected L-leucine according to the method described in our previous publication (**Scheme 1**) [15]. The N-protected amino acids (**4a-4j**; **4a-4c** were commercially available, and **4d-4j** were produced from peptide condensation and hydrolyzation) were coupled with the corresponding α-amino methyl esters **5a-5c** under classic peptide coupling conditions. The obtained dipeptidic methyl esters **6a-6j** were hydrolyzed to give the corresponding acids, followed by coupling with **3** to form compounds **7a-7j** (**Scheme 2**).

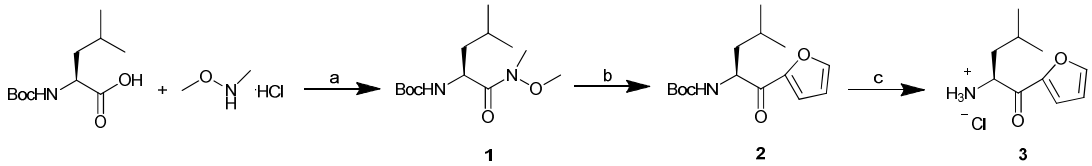

Scheme 1. The synthesis of compound **3**. Reagents and conditions: a) HOBt, EDCI, DMF, NMM, rt, 12 h; b) *n*-BuLi, furan, THF, 0 □, 30 min, then -78□, 2.5 h; c) HCl/dioxane, 0 □, 1 h.

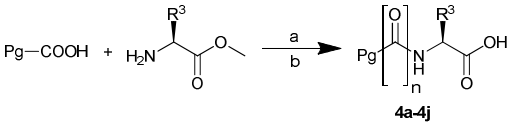

4a R^3= -CH_2(4-OMe)Ph, Pg= Boc, n= 0
4b R^3= -CH_2Ph, Pg= Cbz, n= 0
4c R^3= -CH_2(4-Cl)Ph, Pg= Boc, n= 0
4d R^3= -CH_2(4-OH)Ph, Pg= 4-(hydroxymethyl)phenyl, n= 1
4e R^3= -CH_2Ph, Pg= pyrazin-2-yl, n= 1
4f R^3= -CH_2(4-OMe)Ph, Pg= pyrazin-2-yl, n= 1
4g R^3= -CH_2Ph, Pg= *o*-tolyl, n= 1
4h R^3= -CH_2Ph, Pg= 2-methoxyphenyl, n= 1
4i R^3= -CH_2Ph, Pg= 2-nitrophenyl, n= 1
4j R^3= -CH_2Ph, Pg= 2-bromophenyl, n= 1

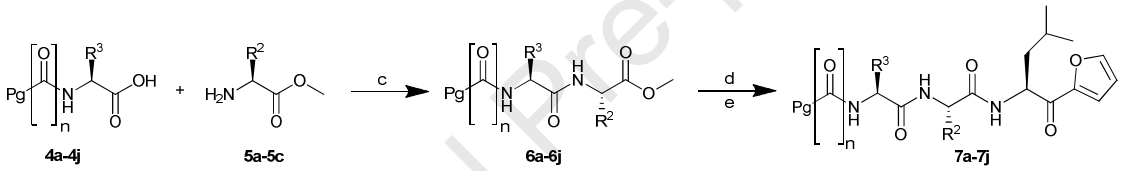

5a R^2 = -CH_2(4-OH)Ph
5b R^2 = -CH_2(4-Cl)Ph
5c R^2 = -CH_2(4-OMe)Ph

6a, **7a** R^2= -CH_2(4-Cl)Ph, R^3= -CH_2(4-OMe)Ph, Pg= Boc, n= 0
6b, **7b** R^2= -CH_2(4-Cl)Ph, R^3= -CH_2Ph, Pg= Cbz, n= 0
6c, **7c** R^2= -CH_2(4-OH)Ph, R^3= -CH_2(4-Cl)Ph, Pg= Boc, n= 0
6d, **7d** R^2= -CH_2(4-OH)Ph, R^3= -CH_2(4-OH)Ph, Pg= 4-(hydroxymethyl)phenyl, n= 1
6e, **7e** R^2= -CH_2(4-OMe)Ph, R^3= -CH_2Ph, Pg= pyrazin-2-yl, n= 1
6f, **7f** R^2= -CH_2(4-OH)Ph, R^3= -CH_2(4-OMe)Ph, Pg= pyrazin-2-yl, n= 1
6g, **7g** R^2= -CH_2(4-OMe)Ph, R^3= -CH_2Ph, Pg= *o*-tolyl, n= 1
6h, **7h** R^2= -CH_2(4-OMe)Ph, R^3= -CH_2Ph, Pg= 2-methoxyphenyl, n= 1
6i, **7i** R^2= -CH_2(4-OMe)Ph, R^3= -CH_2Ph, Pg= 2-nitrophenyl, n= 1
6j, **7j** R^2= -CH_2(4-OMe)Ph, R^3= -CH_2Ph, Pg= 2-bromophenyl, n= 1

Scheme 2. The synthesis of tripeptidic derivatives **7a-7j**. Reagents and conditions: a) HOBt, EDCI, DMF, NMM, rt, 12-24 h; b) 1N LiOH, THF, rt, 2 h; c) HOBt, EDCI, DMF, NMM, rt, 12-24 h; d) 1N LiOH, THF, rt, 2 h; e) **3**, HOBt, EDCI, DMF, NMM, rt, 12-24 h.

The synthesis of **11a-11o** was achieved by a convergent approach (**Scheme 3**) in which N-terminal protected amino acids were coupled to furan-based C-terminal dipeptides. The synthesis of the furylketone dipeptide started from the condensation of L-furan based leucine **3** with N-Boc amino acids through standard amino acid coupling condition. Then, protecting group Boc was removed under acidic condition to give dipeptide hydrochlorides **8a-8c**. The N-terminal tosyl protected amino acids (**10a-10e**) were obtained from free amino acids **9a-9e,** among which **9a-9c** were prepared by deprotection of the N-Boc protected tert-butyl aspartate, and **9d-9e** were commercially available, followed by condensation with p-Tosyl chloride under basic condition.

Finally, the coupling of furan-based C-terminal dipeptides **8a-8c** and the N-terminal protected **10a-10i** (**10f-10i** were commercially available) gave **11a-11o** successfully.

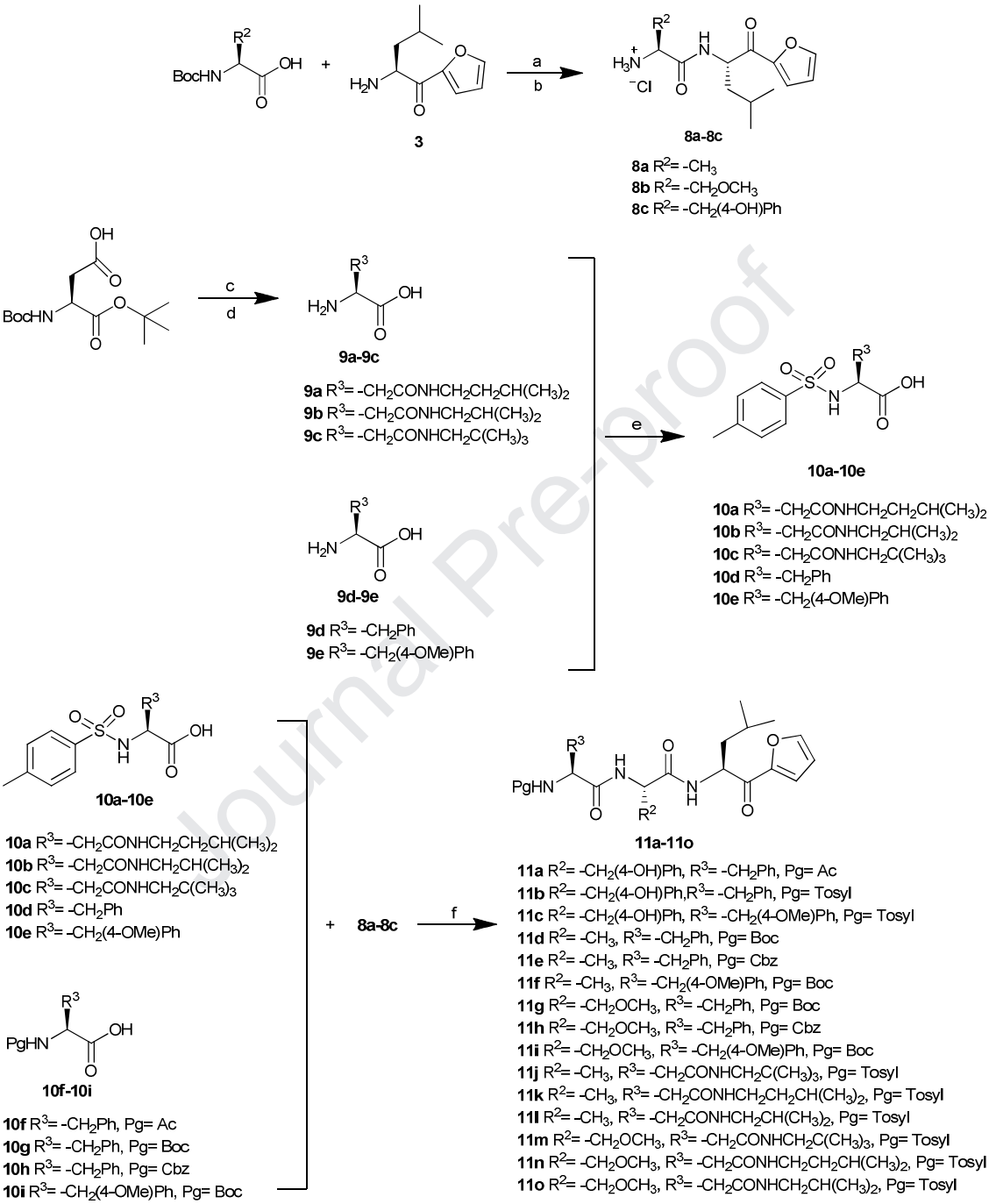

Scheme 3. The synthesis of tripeptidic derivatives **11a-11o**. Reagents and conditions: a) HOBt, EDCI, DMF, NMM, rt, 12-24 h; b) HCl/dioxane, 0□, 1 h; c) amine, HOBt, EDCI, DMF, NMM, rt, 12-24 h; d) HCl/dioxane, 0□, 1 h; e) *p*-Tosyl chloride, NaOH, dioxane; f) HOBt, EDCI, DMF, NMM, rt, 12-24 h.

2.2 Inhibitory activities against human 20S proteasome and SAR analysis

The proteasome inhibitory profiles of synthesized compounds were evaluated on the three active subunits of human 20S proteasome using appropriate luminescent substrates as described in our previous work [15]. None of the compounds displayed > 40% inhibition against β1 and β2 subunits, whereas almost all compounds exhibited good activities toward β5 (CT-L) during primary screening at 50 μM (See **Table S1** in the supporting information). Compounds showed more than 50% inhibition were further evaluated for IC_{50}s, and the results are listed in **Table 1**.

Table 1. Structures and the CT-L activity of proteasome inhibition potencies of target compounds.

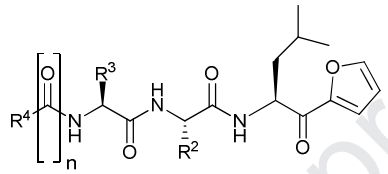

Compd.	R^2	R^3	R^4	n	IC_{50} (μM)[a]
MG132	-	-	-	-	0.11 ± 0.01
11e	CH_3	$PhCH_2$	Cbz	0	> 50
11h	CH_3OCH_2	$PhCH_2$	Cbz	0	4.16 ± 0.23
7b	(4-Cl)$PhCH_2$	$PhCH_2$	Cbz	0	>50
11f	CH_3	(4-OCH_3)$PhCH_2$	Boc	0	11.96 ± 1.88
11i	CH_3OCH_2	(4-OCH_3)$PhCH_2$	Boc	0	5.86 ± 0.67
7a	(4-Cl)$PhCH_2$	(4-OCH_3)$PhCH_2$	Boc	0	49.97 ± 1.93
10b'	(4-OH)$PhCH_2$	(4-OCH_3)$PhCH_2$	Boc	0	1.64 ± 0.44[b]
10d'	(4-OCH_3)$PhCH_2$	(4-OCH_3)$PhCH_2$	Boc	0	8.15 ± 0.11[b]
11d	CH_3	$PhCH_2$	Boc	0	45.61 ± 2.41
11g	CH_3OCH_2	$PhCH_2$	Boc	0	14.27 ± 0.33
7c	(4-OH)$PhCH_2$	(4-Cl)$PhCH_2$	Boc	0	7.26 ± 1.36
11a	(4-OH)$PhCH_2$	$PhCH_2$	Ac	0	13.95 ± 0.54
11b	(4-OH)$PhCH_2$	$PhCH_2$	*p* -tosyl	0	2.33 ± 0.74
7f	(4-OH)$PhCH_2$	(4-OCH_3)$PhCH_2$	pyrazin-2-yl	1	8.25 ± 0.52
7e	(4-OCH_3)$PhCH_2$	$PhCH_2$	pyrazin-2-yl	1	>50
7g	(4-OCH_3)$PhCH_2$	$PhCH_2$	*o*-tolyl	1	3.19 ± 0.17
7h	(4-OCH_3)$PhCH_2$	$PhCH_2$	2-methoxyphenyl	1	>50
7i	(4-OCH_3)$PhCH_2$	$PhCH_2$	2-nitrophenyl	1	7.26 ± 1.94
7j	(4-OCH_3)$PhCH_2$	$PhCH_2$	2-bromophenyl	1	>50
7d	(4-OH)$PhCH_2$	(4-OH)$PhCH_2$	4-(hydroxymethyl)phenyl	1	4.56 ± 0.39
11c	(4-OH)$PhCH_2$	(4-OCH_3)$PhCH_2$	*p* -tosyl	0	0.54 ± 0.10
11j	CH_3	$(CH_3)_3CCH_2NHCOCH_2$	*p*-tosyl	0	5.63 ± 0.72
11l	CH_3	$(CH_3)_2CHCH_2NHCOCH_2$	*p* -tosyl	0	3.12 ± 0.32
11k	CH_3	$(CH_3)_2CHCH_2CH_2NHCOCH_2$	*p* -tosyl	0	6.30 ± 0.35
11m	CH_3OCH_2	$(CH_3)_3CCH_2NHCOCH_2$	*p* -tosyl	0	0.18 ± 0.06
11o	CH_3OCH_2	$(CH_3)_2CHCH_2NHCOCH_2$	*p* -tosyl	0	0.68 ± 0.05

11n	CH_3OCH_2	$(CH_3)_2CHCH_2CH_2NHCOCH_2$	*p* -tosyl	0	>50

[a]Values represent the mean ± SD of three independent experiments, each based on three biological replicates; [b] See reference 15

The substitutions with moderate size at R^2 seemed more preferred when CH_3OCH_2- (e.g. **11h**, **11i**) was compared with -CH_3 (e.g. **11e**, **11f**) or relatively bulky (4-Cl) $PhCH_2$ (e.g. **7b**, **7a**). When 4-Cl (compound **7a**) replaced the electron donating 4-hydroxyl (**10b')** [15] or 4-methoxy (**10d'**) [15] groups on $PhCH_2$, an obvious drop in potency was observed. This seemed also the truth for R^3, as can be seen from the comparison between **7c** and **10b'**.

The contribution of Cbz at R^4 to potency was almost similar (e.g. **11e** *vs* **11d**, **11h** *vs* **11g**) to that of Boc, which was generally consistent with our previous observation, suggesting that there was adequate space to accommodate bulky substitutions for R^4. However, the pyrazin-2-yl that was a privilege N-terminal protecting group used in bortezomib disfavored the activities of furylketone-based tripeptides (**7f** and **7e**). In contrast, *p*-tosyl group was found an efficient N-terminal protecting group (**11b** *vs* **11a**). All together, these results revealed that their order of activities for R^4 are as follows: *p*-tosyl (**11b**) >*o*-tolyl (**7g**) >2-nitrophenyl (**7i**) > acetyl (**11a**) > pyrazin-2-yl (**7e**) > 2-methoxyphenyl (**7h**) ≈ 2-bromophenyl (**7j**), and therefore *p*-tosyl was selected and fixed for R^4 in the following optimizations at R^3. As reported by Pan *et al.* [18], the S^3 sub-pocket prefers to accommodate long and linear side chains. Accordingly, we replaced the rigid $PhCH_2$ with more flexible, as well as bulkier side chains (e.g. **11j**, **11l** and **11k**) for R^3. This attempt was proved successful as the potencies of **11j**, **11l**, and **11k** were comparable to **11b**. The length of the chain at R^3 exhibited great impact on the potency as no inhibition was observed with side chain longer than 7 atoms (compound **11n**). The privileged order of the side chain for R^3 was as follows: 2-neopentylamino-2-oxoethyl (**11m**) > 2-isobutylamino-2-oxoethyl (**11o**) > 2-isopentylamino-2-oxoethyl (**11n**). In summary, the most active compound was found in **11m** which bears the optimal isopropyl group as R^1, methoxymethyl at R^2, 2-neopentylamino-2-oxoethyl for R^3 and *p*-tosyl as the N-terminal protecting group.

The solubility of **11m** was good enough in the aqueous buffers for bio-evaluations, and the IC_{50} of **11m** against β5 subunit was determined as 0.18 ± 0.06 μM which was comparable to that of the positive control MG132 (IC_{50} = 0.11 μM). Nevertheless, its selectivity toward β5 was much higher (showing almost no inhibitory effects on β1 or β2 subunits, **Table S1** in Supporting Information) than MG132 which also inhibits the β1 (IC_{50} = 12.26 μM) and β2 (IC_{50} = 16.30 μM)

subunits. This selectivity may enable less side effects since inhibition of all three subunits might induce a cytotoxic effect on normal cells [19].

2.3 Binding mode analysis

To find out whether **11m** interacts with 20S proteasome in covalent or noncovalent manner, liquid chromatography-tandem mass spectrometry (LC-MS/MS) analyses was carried out to see if covalent modified fragment(s) of 20S proteasome can be found, and to this end, the well-known specific β5 subunit covalent inhibitor, carfilzomib [20], was used as positive control.

As shown in **Figure 3**, the result of vehicle 20S proteasome presented the doubly charged unmodified TTTLAFKFR peptide (m/z 542.8114), corresponding to the N-terminal tryptic peptide of the β5 subunit of human proteasome (**Fig. 3A**). The MW of the peptide fragment covalently modified by **11m** was supposed to increase by about 620 Da. However, the result (**Fig. 3B**) obtained from the sample treated with **11m** was only observed with unmodified TTTLAFKFR peptides (m/z 542.8116, structures shown in **Fig. 3C**). By contrast, a quadruply charged peptide at m/z 451.7651 (**Fig. 3D**) was identified from the sample treated with carfilzomib, corresponding to the carfilzomib-TTTLAFKFR adduct in which carfilzomib was linked with the N-terminal Thr1 (**Fig. 3E**). No modification on other subunits (β1, β2) or other site of β5 subunit of 20S proteasome was identified in the **11m** treated sample according the matching of experimental MWs to the UniProt database.

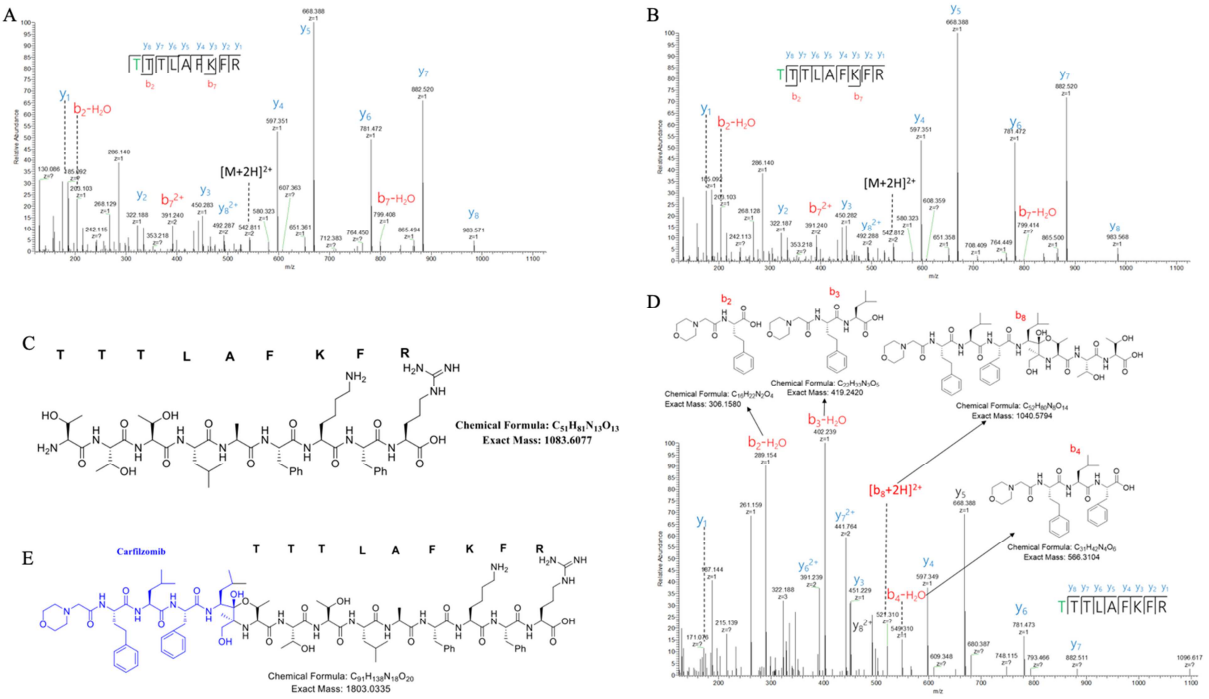

Figure 3. LC-MS/MS analysis of purified human 20S proteasome incubated with vehicle, **11m**, or carfilzomib. (A) Vehicle sample doubly charged unmodified peptide was observed at m/z 542.8114, the tandem mass spectrum of which was matched to peptide TTTLAFKFR (the N-terminal peptide of human 20S proteasome subunit β5); (B) **11m** treated sample, doubly charged unmodified peptide was observed at m/z 542.8116, the tandem mass spectrum of which was matched to peptide TTTLAFKFR; (C) Structure of the unmodified TTTLAFKFKR tryptic peptide; (D) Carfilzomib treated sample, quadruply charged modified peptide was observed at m/z 451.7651, the tandem mass spectrum of which was matched to carfilzomib-modified TTTLAFKFR containing peptide; (E) Structure of the carfilzomib-modified peptide.

The above results suggested that in contrast to carfilzomib, **11m** inhibits 20S proteasome by forming no irreversible covalent modification on it, leaving at least two possibilities regarding binding mode. One is that **11m** interacts with 20S proteasome non-covalently, and the other is that **11m** forms reversible covalent bond.

We next examined the reversibility of the binding between **11m** and 20S proteasome by wash-out assay as described by Sebti *et al.* [21,22]. Compound **10b'**, **11m**, MG132, bortezomib and carfilzomib were pre-incubated with purified human constitutive 20S proteasome and the CT-L inhibitory activity was measured before and after wash-out. As shown in **Figure 4**, the catalytic activity of β5 subunit recovered around 80% in the MG132 or bortezomib treated samples, which was in agreement with the results reported by Tepe *et al.* [23] and Bolen *et al.* [24] that they were reversible covalent inhibitors. Carfilzomib was irreversible with only 10% catalytic activity recovery as reported by Bennett *et al.* [25].

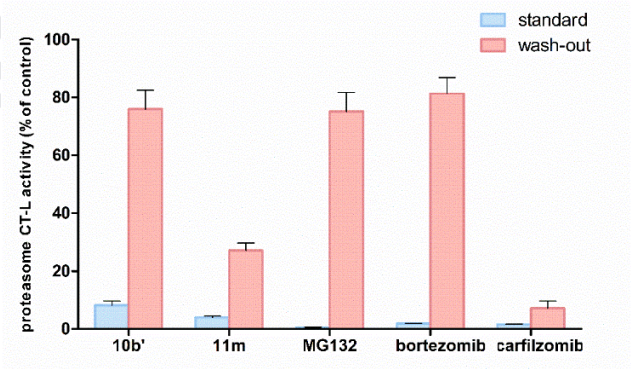

Figure 4. CT-L activity of the human 20S proteasome treated with **10b'**, **11m**, MG132, bortezomib or carfilzomib before and after wash-out.

Similar to MG132 and bortizomib, the CT-L activity of the sample treated with **10b'** significantly recovered (>70%) after wash-out, which was consistent with our former observation in dynamic simulations that **10b'** formed no covalent bond due to torsion constraint [15].

However, unlike **10b'**, the sample treated with **11m** only exhibited very low activity recovery (< 30% active) suggesting a limited reversibility regarding binding. This observation partially supported our hypothesis that the furyl ketone warhead was electrophilic to interact with the catalytic Thr1 of β5 subunit by forming hemiketal which endowed the inhibition with reversibility due to the slow hydrolysis of the hemiketal intermediate (**Fig. 5**).

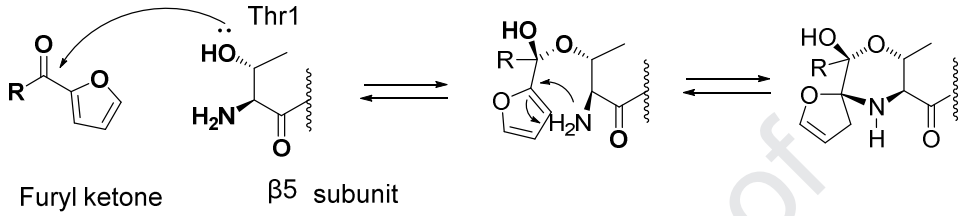

Figure 5. The hypothesized covalent interaction between furyl ketone warhead and the catalytic Thr1 of the β5 subunit of human 20S proteasome

Although the covalent modification of **11m** on 20S proteasome was hard to be identified by LC-MS/MS, the formation of hemiketal of compound **11m** could be observed in high performance liquid chromatography (HPLC) in considerable amount (~ 27%) as peaks separate from the main product using H_2O-MeOH as mobile phase. However, the small peak of methyl hemiketal was absent when the sample was eluted with H_2O-CH_3CN system.

2.4 Molecular docking analysis of 11m.

In order to find out the binding mode of **11m** with proteasome, we docked compound **11m** into the β5 subunit of 20S proteasome isolated from its complex with a peptidic inhibitor (PDB code: 4NO8) using Gold 3.0.1 software. As depicted in **Fig. 6A**, the tripeptide backbone of **11m** generated an anti-parallel β-sheet conformation, making essential hydrogen bonds with β5 (**Thr 21**, **Gly 47**, **Ala 49**) and β6 (**Asp 126**) subunits. In this binding conformation, **11m** closely resembled the native ligand of **4NO8** (ligand 6) with its peptidomimetic chain [26], although the side chains slightly differ in their orientations (**Fig. 6B**). Besides, **11m** also provide the opportunity to partially exploit the S1' specific pocket by protruding its C-terminal moiety like ligand **6** does. The distance between the Thr1O^{γ} and the furylketone moiety was 2.4 Å (**Fig. 6A**), which was prerequisite for hemiketal formation and in agreement with our previous SAR discussion and LC-MS/MS results.

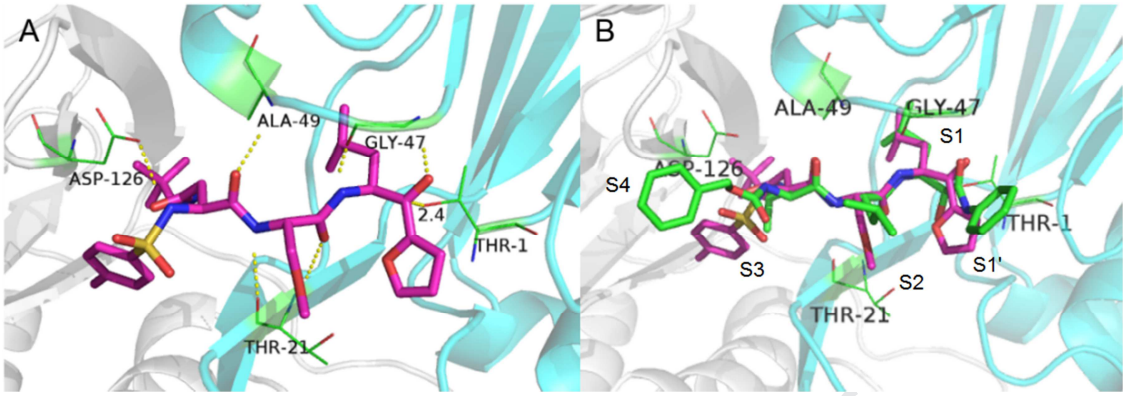

Figure 6. (A) Predicted binding mode of compound **11m** (magenta) into the β5 (cyan)/β6 (light grey) active site of the 20S proteasome (PDB code: 4NO8); key hydrogen bonds between the inhibitor and protein are shown as yellow dashed lines; the distance between the carbonyl carbon atom of the furyl ketone group and the hydroxy oxygen atom of Thr1 is marked, the value is 2.4 Å. (B) Superposition of **11m** with the native ligand **6** (green) of the complex (4NO8) within β5 (cyan)/β6 (white) active site of 20S proteasome.

2.5 Binding kinetics analysis through Surface Plasmon Resonance

We next measured the binding affinity of **11m** with purified human 20S proteasome through surface plasmon resonance (SPR) on a GE Biacore T200 apparatus. As shown in **Figure 7**, both MG132 and **11m** evoked specific binding and dose-dependent responses to CM5 chip [27] linked with purified human 20S proteasome. Based on a 1:1 langmuir binding mode fit [28], the equilibrium dissociation constants (K_D) calculated from the K_a/K_d ratio for MG132 and **11m** were 17μM and 4.8 μM respectively, indicating a higher binding affinity of **11m** than MG132 to 20S proteasome. Furthermore, **11m** had also shown a significantly slower dissociation rate than MG132 (**Table 2**) indicating a prolonged acting time of **11m**, and the relatively "rapid binding and slow dissociation" profile of **11m** was supposed to be beneficial in case used *in vivo* due to reduced dosing frequency.

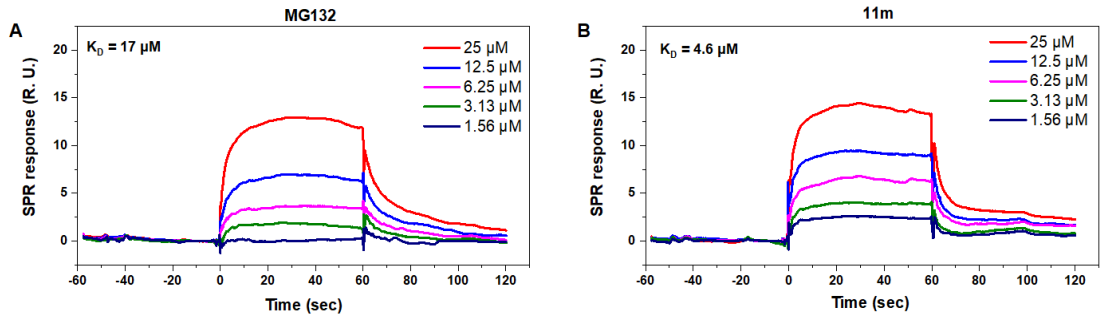

Figure 7. SPR sensorgram of (A) MG132 and (B) **11m** binding to 20S proteasome immobilized on a CM5 chip.

Table 2. Association (K_a), and dissociation (K_d) rate constants determined by SPR

Compd.	K_a(1/Ms)	K_d(1/s)	K_D (μM)
MG132	2716	0.04609	17
11m	4209	0.01922	4.8

2.6 Measurement of Anti-proliferative Effects on Cancer Cell Lines

Three most potent compounds (**11c, 11m** and **11o**) were selected for the test against a panel of human cancer cell lines, including malignant melanoma, colorectal adenocarcinoma, and lung carcinoma, etc. The anti-proliferation effects were measured by CellTiter-Glo® Luminescent Cell Viability Assay (Promega Inc. Cat. # G7570) [15], and the results are summarized in **Table 3.** As expected, the best potency was also achieved by **11m**, which was in line with the enzymatic assay (**Table 1**). Compound **11m** exhibited good anti-proliferative effect which was comparable to MG132 among all tested cancer cell lines. Interestingly, **11m** was also found showing similar single-digit micromolar IC_{50} as in the enzymatic assay.

Notably, the anti-proliferation effect was significant in fast proliferating cancer cells, while the nonmalignant cell (HEK293) remained unaffected with IC_{50} values greater than 50 μM. This specificity toward cancer cells promises that normal cells will not be affected when used *in vivo*.

Table 3. Cytotoxicity of selected compounds against a panel of solid cancer cell lines or nonmalignant cell line.

Compd.	IC_{50} (μM) [a]							
	A375	BGC-823	Hela	HT-29	A549	PC3M1E8	HCT-116	HEK293
11c	3.87 ± 1.32	8.37 ± 1.36	6.35 ± 3.10	5.40 ± 3.15	13.07 ± 3.48	4.98 ± 3.82	3.52 ± 1.94	>50
11m	0.88 ± 0.37	0.77 ± 0.28	0.67 ± 0.08	0.73 ± 0.03	1.30 ± 0.17	0.57 ± 0.22	0.28 ± 0.13	>50
11o	2.61 ± 0.13	3.96 ± 0.45	2.47 ± 0.30	4.85 ± 0.81	17.59 ± 6.43	3.73 ± 1.88	1.67 ± 0.44	>50
MG132	0.59 ± 0.06	1.00 ± 0.12	0.71 ± 0.13	0.78 ± 0.31	0.70 ± 0.02	0.96 ± 0.06	0.40 ± 0.03	>50

[a]Values represent the mean ± SD of three independent experiments, each based on three biological replicates.

2.7 Measurement of Effects on Cell Cycle.

To further validate the anti-proliferative effects of our furylketone derivatives, the cell cycle arrest effects were analyzed by flow cytometry taking **11c**, **11m**, and **11o** as representatives, in which HCT-116 cells were first treated with either vehicle or compound before harvested and

stained with propidium iodide for analysis. As shown in **Figure 8**, compound **11c**, **11m**, and **11o** had arrested the cell cycle at G2/M phase at a concentration as low as 1 μM, just like MG132 did. The highest percentage of cell population at G2/M phase was observed in the **11m** treated group which was in agreement with its good potency in both enzymatic and cellular assays. Therefore, compound **11m** was selected for further *in vivo* investigations as anti-tumor agent.

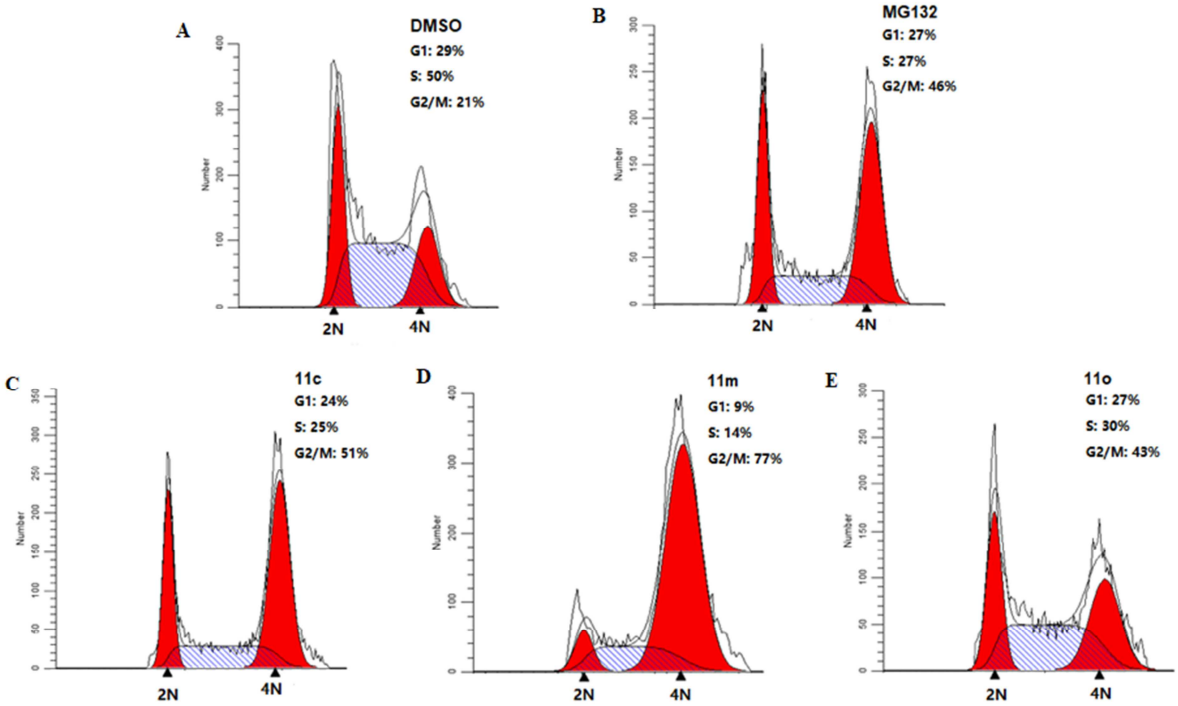

Figure 8. Human colorectal cancer cell line HCT-116 cells were treated with either vehicle, MG132, **11c**, **11m**, or **11o** for 24 hours. The cells were stained with propidium iodide and analyzed by fluorescence activated cell sorting to measure cellular chromosomal DNA content. Population distributions of HCT-116 cells treated with 1 μM of (A) DMSO, (B) MG132, (C) **11c**, (D) **11m**, or (E) **11o**.

2.8 Pharmacokinetic (PK) Evaluations of Compound 11m

The *in vivo* pharmacokinetic (PK) profiles of compound **11m** were analyzed in rats. The concentrations of **11m** in plasma were measured after a single dose of intravenous injection (5 mg/kg). The key pharmacokinetic parameters of compound **11m** are summarized in **Table 4**. In rats, **11m** was rapidly cleared from the plasma following *i.v.* administration with an average terminal plasma half-life of ~14 min, similar to carfilzomib (~17 min) [29] that also possesses a tripeptidic backbone.

Table 4. Pharmacokinetic parameters of **11m**

Administrations	C_{max} (μg/L)	AUC_{0-t} (μg/L·h)	$T_{½}$ (min)	MRT (min)	CL (L/h/kg)	V_{ss} (L/kg)
11m (iv, 5 mg/kg)	2007 ± 240	680 ± 173	13.83 ± 1.80	20.20 ± 1.05	2.0 ± 0.46	0.66 ± 0.01
Carfilzomib (iv, 4 mg/kg)[29]	27824 ± 2304	343 ± 22	17 ± 9		11.7 ± 0.72	0.3 ± 0.1

The area under the concentration-time curve (AUC_{0-t}) of compound **11m** was about 680 μg/L·h which was twice larger than that of carfilzomib (343 μg/L·h), indicating a broader tissue distribution *in vivo*. In addition, compound **11m** achieved a maximum plasma concentration (C_{max}) of 2007 μg/L within about 5 min and a volume of distribution at steady state (Vss) of 0.66 L/kg, which was much larger than blood volume (69 mL/kg in male rats) [30], suggesting extensive tissue permeability which endow it with the possibility to be used for the treatment of solid tumors in addition to multiple myeloma and other neoplastic hematologic disorders. Moreover, **11m** showed a lower clearance rate (CL) of 2.0 L/h/kg. These results indicated that **11m** might penetrate extensively into peripheral tissues and was largely eliminated extrahepatically [20].

2.9 *In vivo* anti-tumor activity of 11m

To assess the *in vivo* antitumor efficacy of compound **11m**, HCT-116 cell xenograft nude mice model was used. Mice bearing palpable tumor were divided into 3 groups and treated with vehicle, carfilzomib (5 mg/kg) or **11m** (10 mg/kg), respectively via intravenous injection twice weekly for consecutive four weeks.

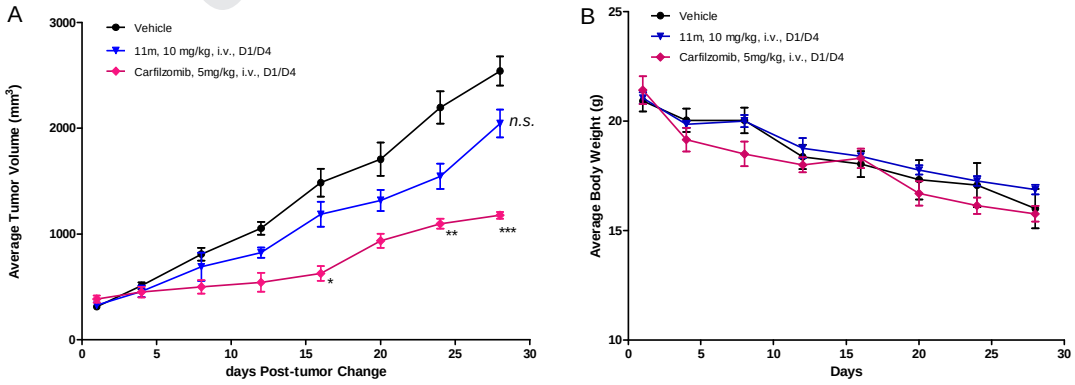

Figure 9. 11m inhibits tumor growth *in vivo*. Male nude mice bearing HCT-116 tumors received **11m,** carfilzomib or vehicle alone (n= 3 mice/group). Results are expressed as mean±SEM. (A) Tumor growth curves in animals receiving the respective treatments (*n.s.*, non-significant; * , P < 0.05 ; ** , P < 0.01 ; *** , P < 0.001,

significantly different from control group, two-way ANOVA followed by Bonferroni post tests); (B) Average body weights of mice receiving the respective treatments (non-significantly different for both Carfilzomib and **11m** groups compared with control group, two-way ANOVA followed by Bonferroni post tests).

As shown in **Fig. 9A**, carfilzomib could inhibit tumor growth *in vivo* and exhibited significant difference ($P < 0.001$) comparing to the vehicle treated group after 28 days' treatment. Although no statistically significant difference was observed during the treatment, **11m** also reduced tumor progression, albeit to a lesser extent than carfilzomib. The body weight of both carfilzomib and **11m** group did not significantly drop over the period of treatment compared with the vehicle group (**Fig. 9B**), indicating **11m** was well tolerated in mice without apparent systemic toxicity. The present findings suggest that **11m** demonstrates weak antitumor activity towards solid tumor *in vivo*.

3.Conclusion

We designed and synthesized a series of tripeptidic furylketones as 20S proteasome inhibitors that selectively inhibited the CT-L activity. The results of LC-MS/MS analyses and wash-out assay indicated they inhibit the β5 subunit in reversible manner. Docking study suggested the distance between the C-terminal furylketone moiety and the catalytic Thr1 allowed the formation of hemiketal which endow these furylketones "rapid loading and slow dissociation" kinetics. Although not as potent as carfilzomib to inhibit tumor growth in tumor xenograft model mice, the most active compound **11m** exhibited greater tissue distribution and much lower plasma clearance indicating the potential of these inhibitors to combat solid tumors when administrated in an optimized dosing regimen.

4.Experimental Section

4.1 Chemistry

Commercially available solvents and reagents were used directly without further purification. Reaction progress was monitored by thin-layer chromatography (TLC) performed on silica gel GF254 purchased from Qingdao Haiyang Chemical Co. (Qingdao, China). Melting points (mp) were obtained on an XT4A apparatus and were uncorrected. ^{1}H NMR and ^{13}C NMR spectra were recorded at 400/100 MHz on a Bruker Avance III 400 spectrometer with TMS as

internal standard. Low-resolution mass spectra were obtained using a Waters ACQ-SQD LC–MS instrument in electrospray positive and negative ionization modes. High-resolution mass spectrometry (HRMS) data were recorded on a Bruker APEX IV FTMS system. For all final compounds, analytical reverse phase HPLC was run using an Agilent 1260 series instrument equipped with an Eclipse Plus C18 column (3.5 μm, 4.6×100 μm) at a flow rate of 1 mL min^{-1} and a gradient of solvent A (water) and solvent B (acetonitrile). HPLC results showed that the purity of all the final products was greater than 95%.

The intermediates **3**, **4a-4j** and **6a-6j** were synthesized according to our previous reported methods [15]. Detailed synthesis and structural characterization data of other compounds are indicated below.

4.1.1 tert-butyl-((S)-1-(((S)-3-(4-chlorophenyl)-1-(((S)-1-(furan-2-yl)-4-methyl-1-oxopentan-2-yl)amino)-1-oxopropan-2-yl)amino)-3-(4-methoxyphenyl)-1-oxopropan-2-yl)carbamate (7a): 1N LiOH was added to a solution of **6a** in THF until pH 12-13, and the reaction mixture was stirred at room temperature for 2 h, followed by acidification with 1N HCl until pH 2-3. The aqueous phase was extracted with EtOAc (5×10 mL), and the combined organic phases were dried with Na_2SO_4. The solvent was concentrated in vacuo, and the resulting residue was used in the next step without further purification. EDC·HCl (230 mg, 1.2 mmol) and HOBt (162 mg, 1.2 mmol) were added to a solution of the crude acid obtained previously (1 mmol), and **3** (217 mg, 1 mmol) in the presence of NMM (0.34 mL, 3 mmol) in 10 mL DMF. The reaction mixture was stirred at room temperature overnight and diluted with EtOAc and washed with 10% citric acid, saturated aqueous $NaHCO_3$ and brine, dried with Na_2SO_4, and concentrated *in vacuo* to give the crude product, which was separated by silica gel chromatography to yield **7a** as a white solid (495 mg, 77%); mp: 176-177 □; ^{1}H NMR (400 MHz, DMSO-d_6): δ = 0.89-0.92 (m, 6H, CH_3), 1.28 (s, 9H, Boc), 1.49-1.55 (m, 2H, CH_2), 1.64-1.67 (m, 1H, CH), 2.54-2.60 (m, 1H, CH_2Ph), 2.75-2.78 (m, 2H, CH_2Ph), 2.94-2.98 (m, 1H, CH_2Ph), 3.70 (s, 3H, OCH_3), 4.01-4.06 (m, 1H, CH), 4.57-4.62 (m, 1H, CH), 5.00-5.06 (m, 1H, CH), 6.74 (dd, *J* = 1.4, 3.4 Hz, 1H, F-4), 6.78-6.82 (m, 3H, Ph, NH), 7.08 (d, *J* = 8.4 Hz, 2H, Ph), 7.19-7.26 (m, 4H, Ph), 7.47 (d, *J* = 3.6 Hz, 1H, F-3), 7.95 (d, *J* = 8.6 Hz, 1H, NH), 8.05 (s, 1H, F-5), 8.50 ppm (d, *J* = 7.6 Hz, 1H, NH); ^{13}C NMR (100 MHz, DMSO-d_6): δ = 21.9, 23.5, 24.9, 28.6, 37.1, 37.6, 39.4, 39.6, 39.8, 40.0, 40.2, 40.4, 40.6, 52.9, 53.5, 55.4, 56.5, 78.6, 113.1, 113.9, 119.5, 128.3, 130.3, 130.6, 131.5, 131.6,

136, 148.7, 150.8, 155.5, 158.2, 171.1, 171.9, 187.5 ppm; HRMS (ESI) *m/z* $[M+H]^+$ calcd for $C_{34}H_{43}ClN_3O_7$: 640.27840, found: 640.27683; HPLC: t_R= 10.29 min (96.4% purity).

4.1.2 benzyl-((S)-1-(((S)-3-(4-chlorophenyl)-1-(((S)-1-(furan-2-yl)-4-methyl-1-oxopentan-2-yl)amino)-1-oxopropan-2-yl)amino)-1-oxo-3-phenylpropan-2-yl)carbamate (7b):

Following the same procedure as described for the synthesis of **7a** except for starting from **6b**, **7b** was obtained in 67% yield as a white solid; mp: 184-185□; ^{1}H NMR (400 MHz, DMSO-d_6): δ = 0.90-0.93 (m, 6H, CH_3), 1.46-1.58 (m, 2H, CH_2), 1.60-1.67 (m, 1H, CH), 2.65 (dd, *J* = 11.1, 13.6 Hz, 1H, CH_2Ph), 2.77 (dd, *J* = 9.0, 22.7 Hz, 1H, CH_2Ph), 2.90 (dd, *J* = 3.8, 14.0 Hz, 1H, CH_2Ph), 2.98 (dd, *J* = 4.8, 18.6 Hz, 1H, CH_2Ph), 4.20-4.25 (m, 1H, CH), 4.57-4.62 (m, 1H, CH), 4.93 (s, 2H, OCH_2Ph), 5.01-5.06 (m, 1H, CH), 6.73-6.74 (dd, *J* = 1.5, 3.4 Hz, 1H, F-4), 7.18-7.33 (m, 14H, Ph), 7.44 (d, *J* = 8.8 Hz, 1H, NH), 7.47 (d, *J* = 3.5 Hz, 1H, F-3), 8.05 (s, 1H, F-5), 8.13 (d, *J* = 8.2 Hz, 1H,NH), 8.48 ppm (d, *J* = 7.6 Hz, 1H, NH); ^{13}C NMR (100 MHz, DMSO-d6): δ = 21.9, 23.5, 24.9, 37.4, 37.9, 39.4, 39.6, 39.8, 40.0, 40.2, 40.4, 40.6, 53.0, 53.7, 56.5, 65.7, 113.1, 119.5, 126.7, 127.9, 128.1, 128.4, 128.5, 128.7, 129.6, 131.5, 131.6, 136.9, 137.4, 138.5, 148.7, 150.8, 156.2, 171.1, 171.7, 187.5 ppm; HRMS (ESI) *m/z* $[M+H]^+$ calcd for $C_{36}H_{39}ClN_3O_6$: 644.25219, found: 644.25203; HPLC: t_R = 10.45 min (96.9% purity).

4.1.3 tert-butyl-((S)-3-(4-chlorophenyl)-1-(((S)-1-(((S)-1-(furan-2-yl)-4-methyl-1-oxopentan-2-yl)amino)-3-(4-hydroxyphenyl)-1-oxopropan-2-yl)amino)-1-oxopropan-2-yl)carbamate (7c): Following the same procedure as described for the synthesis of **7a** except for starting from **6c**, **7c** was obtained in 76% yield as a white solid; mp: 127□; ^{1}H NMR (400 MHz, DMSO-d_6): δ = 0.89-0.92 (m, 6H, CH_3), 1.28 (s, 9H, Boc), 1.45-1.57 (m, 2H, CH_2), 1.62-1.67 (m, 1H, CH), 2.62-2.68 (m, 2H, CH_2Ph), 2.83-2.88 (m, 2H, CH_2Ph), 4.02-4.11 (m, 1H, CH), 4.48-4.53 (m, 1H, CH), 5.00-5.05 (m, 1H, CH), 6.59 (d, *J* = 8.3 Hz, 2H, Ph), 6.73 (dd, *J* = 1.5, 3.5 Hz, 1H, F-4), 6.90 (d, *J* = 8.9 Hz, 1H, NH), 6.97 (d, *J* = 8.2 Hz, 2H, Ph), 7.18 (d, *J* = 8.3 Hz, 2H, Ph), 7.28 (d, *J* = 8.2 Hz, 2H, Ph), 7.46 (d, *J* = 3.6 Hz, 1H, F-3), 7.88 (d, *J* = 8.2 Hz, 1H, NH), 8.04 (s, 1H, F-5), 8.45 (d, *J* = 7.7 Hz, 1H, NH), 9.13 ppm (s, 1H, OH); ^{13}C NMR (100 MHz, DMSO-d_6): δ = 21.9, 23.5, 24.8, 28.5, 31.4, 37.4, 39.4, 39.6, 39.8, 40.0, 40.2, 40.4, 40.6, 52.9, 54.1, 56.1, 78.6, 113.1, 115.3, 119.5, 127.8, 128.3, 130.6, 131.3, 131.5, 137.6, 148.6, 150.9, 155.5, 156.3, 171.4, 187.5 ppm; HRMS (ESI) *m/z* $[M+H]^+$ calcd for $C_{33}H_{41}ClN_3O_7$: 626.26275, found: 626.26338; HPLC: t_R = 9.20 min (97.8% purity).

4.1.4 N-((S)-1-(((S)-1-(((S)-1-(furan-2-yl)-4-methyl-1-oxopentan-2-yl)amino)-3-(4-hydroxyphenyl)-1-oxopropan-2-yl)amino)-3-(4-hydroxyphenyl)-1-oxopropan-2-yl)-4-(hydroxymethyl)benzamide (7d): Following the same procedure as described for the synthesis of **7a** except for starting from **6d**, **7d** was obtained in 49% yield as a white solid; mp: 161□; ^{1}H NMR (400 MHz, DMSO-d_6): δ = 0.90 (dd, J = 4.7, 10.0 Hz, 6H, CH_3), 1.45-1.68 (m, 3H, CH_2, CH), 2.62-2.70 (m, 2H, CH_2), 2.76-2.92 (m, 2H, CH_2), 4.48-4.54 (m,4H, CH_2, CH), 4.96-5.06 (m,1H, CH), 5.28 (s, 1H, NH), 6.55 (dd, J = 3.6, 8.1 Hz, 2H, Ph), 6.59 (dd, J = 3.7, 8.1 Hz, 2H, Ph), 6.72 (s,1H, F-4), 6.96-7.07 (m, 4H, Ph), 7.36 (t, J = 5.6 Hz, 2H, Ph), 7.47 (t, J = 3.6 Hz, 1H, F-3), 7.73 (d, J = 7.3 Hz, 2H, Ph), 8.03 (s, 2H, F-5, NH), 8.30-8.41 (m,2H, NH, OH), 9.10 ppm (d, J = 4.7 Hz, 2H, OH); ^{13}C NMR (100 MHz, DMSO-d_6): δ = 21.9, 23.5, 24.8, 36.9, 37.2, 37.3, 53.1, 54.4, 55.7, 62.9, 113.1, 115.2, 119.5, 126.3, 127.7, 128.0, 128.2, 128.8, 130.5, 130.7, 132.8 , 146.5, 148.6, 150.8, 156.1, 156.2, 166.6, 171.5, 171.8, 187.7 ppm; HRMS (ESI) *m/z* $[M+H]^+$ calcd for $C_{36}H_{40}N_3O_8$: 642.28099, found: 642.27997; HPLC: t_R = 8.38 min (96.6% purity).

4.1.5 N-((S)-1-(((S)-1-(((S)-1-(furan-2-yl)-4-methyl-1-oxopentan-2-yl)amino)-3-(4-methoxyphenyl)-1-oxopropan-2-yl)amino)-1-oxo-3-phenylpropan-2-yl)pyrazine-2-carboxamide (7e): Following the same procedure as described for the synthesis of **7a** except for starting from **6e**, **7e** was obtained in 69% yield as a white solid; mp: 165-166□; ^{1}H NMR (400 MHz, DMSO-d_6): δ= 0.90 (d, J = 6.6 Hz, 3H, CH_3), 0.93 (d, J = 6.5 Hz, 3H, CH_3), 1.47-1.61 (m, 2H, CH_2), 1.63-1.72 (m, 1H, CH), 2.67-2.72 (m, 1H, CH_2Ph), 2.91-2.95 (m, 1H, CH_2Ph), 3.01-3.10 (m, 2H, CH_2Ph), 3.64 (s, 3H, OCH_3), 4.56-4.62 (m, 1H, CH), 4.74-4.79 (m, 1H, CH), 5.04-5.09 (m, 1H, CH), 6.70 (d, J = 8.5 Hz, 2H, Ph), 6.74 (dd, J = 1.6, 3.5 Hz, 1H, F-4), 7.11-7.17 (m, 7H, Ph), 7.49 (d, J = 3.5 Hz, 1H, F-3), 8.05 (d, J = 0.8 Hz, 1H, F-5), 8.40 (d, J = 8.5 Hz, 1H, NH), 8.52 (d, J = 7.7 Hz, 1H, NH), 8.63 (d, J = 8.6 Hz, 1H, NH), 8.72 (d, J = 1.5 Hz, 1H, P-5), 8.87 (d, J = 2.2 Hz, 1H, P-6), 9.12 ppm (d, J = 1.0 Hz, 1H, P-3); ^{13}C NMR (100 MHz, DMSO-d_6): δ = 21.9, 23.5, 24.9, 37.4, 37.9, 39.4, 39.6, 39.8, 40.0, 40.2, 40.4, 40.6, 52.9, 54.1, 54.3, 55.3, 113.1, 113.8, 119.5, 126.8, 128.4, 129.7, 130.6, 137.7, 143.8, 143.9, 144.4,148.3, 148.7, 150.8, 158.2, 162.5, 170.4, 171.4, 187.5 ppm; HRMS (ESI) *m/z* $[M+H]^+$ calcd for $C_{34}H_{38}N_5O_6$: 612.28166, found: 612.28120; HPLC: t_R = 8.27 min (99.7% purity).

4.1.6 N-((S)-1-(((S)-1-(((S)-1-(furan-2-yl)-4-methyl-1-oxopentan-2-yl)amino)-3-(4-hydroxyphenyl)-1-oxopropan-2-yl)amino)-3-(4-methoxyphenyl)-1-oxopropan-2-yl)pyrazine-2-carboxamide (7f): Following the same procedure as described for the synthesis

of **7a** except for starting from **6f**, **7f** was obtained in 59% yield as a white solid; mp: 115-116□; ^{1}H NMR (400 MHz, DMSO-d_6): δ = 0.83-0.95 (m, 6H, CH_3), 1.49-1.59 (m, 2H, CH_2), 1.64-1.73(m, 1H, CH), 2.66 (dd, J = 9.6,13.8 Hz, 1H, CH_2), 2.87-3.02 (m,3H, CH_2),3.67 (s, 3H, CH_3), 4.54-4.61 (m,1H, CH), 4.69-4.76 (m,1H, CH), 5.05-5.11 (m,1H, CH), 6.55-6.64 (m, 2H, Ph), 6.68-6.79 (m, 3H, Ph, F-4), 7.04 (dd, J = 8.6, 16.7 Hz, 4H, Ph), 7.49 (d, J = 3.5 Hz, 1H, F-3), 8.04 (d, J = 0.8 Hz, 1H, F-5), 8.38 (d, J = 8.4 Hz, 1H, NH), 7.51 (d, J = 7.6 Hz, 1H, NH), 8.61 (d, J = 8.5 Hz, 1H, NH), 8.72 (s, 1H, OH), 8.88 (d, J = 2.36 Hz, 1H, P-5), 9.12 ppm (d, J = 7.2 Hz, 2H, P-6, P-3); ^{13}C NMR (100 MHz, DMSO-d_6): δ = 21.9, 23.5, 24.9, 37.1, 37.4, 53.0, 54.3, 55.3, 113.1, 113.9, 115.3, 119.5, 128.0, 129.4, 130.5, 130.8, 143.8, 143.9, 144.5, 148.3, 148.6, 148.7, 150.8, 156.2, 158.3, 162.5, 170.4, 171.6, 187.6 ppm; HRMS (ESI) *m/z* [M+H]$^+$ calcd for $C_{34}H_{38}N_5O_7$: 628.2785, found: 628.2781; HPLC: t_R = 9.62 min (99.0% purity).

4.1.7 N-((S)-1-(((S)-1-(((S)-1-(furan-2-yl)-4-methyl-1-oxopentan-2-yl)amino)-3-(4-methoxyphenyl)-1-oxopropan-2-yl)amino)-1-oxo-3-phenylpropan-2-yl)-2-methylbenzamide (7g): Following the same procedure as described for the synthesis of **7a** except for starting from **6g**, **7g** was obtained in 84% yield as a white solid; mp: 152-154□; ^{1}H NMR (400 MHz, DMSO-d_6): δ = 0.91 (dd, J = 6.6, 10.0 Hz, 6H, CH_3), 1.50-1.70 (m, 3H, CH_2, CH), 2.04 (d, J = 5.0 Hz, 3H, CH_3), 2.62-3.05 (m,4H, CH_2), 3.66 (d, J = 8.3 Hz, 3H, OCH_3), 4.62-4.71 (m, 2H, CH), 5.07 (s,1H, CH), 6.75 (s, 3H, Ph, F-4), 7.06-7.29 (m, 11H, Ph), 7.50 (s, 1H, F-4), 8.00-8.39 (m, 3H, F-3, NH), 8.51 ppm (t, J = 7.2, 14.2 Hz, 1H, NH); ^{13}C NMR (100 MHz, DMSO-d6): δ = 19.5, 21.9, 23.5, 24.9, 37.4, 52.9, 53.2, 54.1, 54.8, 55.3, 113.1, 113.9, 119.6, 125.7, 126.7, 127.3, 128.5, 129.6, 129.7, 130.7, 135.8, 137.1, 138.6, 148.7, 150.9, 158.3, 169.3, 171.4, 171.6, 187.5, 187.7 ppm; HRMS (ESI) *m/z* [M+H]$^+$ calcd for $C_{37}H_{42}N_3O_6$: 624.3074, found: 624.3079; HPLC: t_R = 9.47 min (99.5% purity).

4.1.8 N-((S)-1-(((S)-1-(((S)-1-(furan-2-yl)-4-methyl-1-oxopentan-2-yl)amino)-3-(4-methoxyphenyl)-1-oxopropan-2-yl)amino)-1-oxo-3-phenylpropan-2-yl)-2-methoxybenzamide (7h): Following the same procedure as described for the synthesis of **7a** except for starting from **6h**, **7h** was obtained in 75% yield as a white solid; mp: 103-105□; ^{1}H NMR (400 MHz, DMSO-d_6): δ = 0.86-0.95 (m, 6H, CH_3), 1.49-1.69 (m, 3H, CH_2, CH), 2.04 (d, J = 5.0 Hz, 3H, CH_3), 2.64-3.10(m, 4H, CH_2), 3.66 (s, 3H, CH_3), 3.77 (s, 3H, OCH_3), 4.51-4.62 (m, 1H, CH), 4.71-4.80 (m, 1H, CH), 5.00-5.11(m, 1H, CH), 6.71-6.82(m, 4H, Ph), 7.01-7.23 (m, 8H, Ph), 7.46-7.49(m, 2H, F-4, Ph), 7.78-7.83 (m, 1H, F-3), 7.78-7.83 (m, 1H, F-3), 8.04 (d, J =

8.4 Hz, 1H, NH), 8.22-8.29 (m, 1H, F-5), 8.45-8.49 ppm (m, 2H, NH); ^{13}C NMR (100 MHz, DMSO-d6): δ = 21.9, 23.4, 24.9, 37.1, 38.1, 53.2, 54.2, 54.5, 55.4, 56.4, 112.7, 113.1, 114.0, 119.4, 121.1, 121.9, 126.7, 128.3, 129.8, 130.1, 130.6, 131.3, 133.3, 137.4, 148.6, 150.9, 157.7, 158.2, 164.3, 170.9, 171.7, 187.7 ppm; HRMS (ESI) *m/z* $[M+H]^+$ calcd for $C_{37}H_{42}N_3O_7$: 640.3023, found: 640.3018; HPLC: t_R = 9.46 min (99.7% purity).

4.1.9 N-((S)-1-(((S)-1-(((S)-1-(furan-2-yl)-4-methyl-1-oxopentan-2-yl)amino)-3-(4-methoxyphenyl)-1-oxopropan-2-yl)amino)-1-oxo-3-phenylpropan-2-yl)-2-nitrobenzamide (7i): Following the same procedure as described for the synthesis of **7a** except for starting from **6i**, **7i** was obtained in 89% yield as a white solid; mp: 193-195□; ^{1}H NMR (400 MHz, DMSO-d_6): δ = 0.89 (d, *J* = 6.6 Hz, 3H, CH_3), 0.92 (d, *J* = 6.5 Hz, 3H, CH_3), 1.45-1.59 (m, 2H, CH_2), 1.63-1.67 (m, 1H, CH), 2.72-2.86 (m, 2H, CH_2), 2.95 (dd, *J* = 4.9, 14.0 Hz, 1H, CH), 3.00 (dd, *J* = 4.0, 14.0 Hz, 1H, CH), 3.68 (s, 3H, CH_3), 4.54-4.61 (m, 1H, CH), 4.67-4.73 (m, 1H, CH), 5.02-5.08 (m, 1H, CH), 6.73-6.76 (m, 3H, Ph, F-4), 7.12 (d, *J* = 8.4 Hz, 2H, Ph), 7.18-7.22 (m, 1H, Ph), 7.26-7.33 (m, 5H, Ph), 7.48(d, *J* = 3.4 Hz, 1H, F-3), 7.66 (t, *J* = 7.8 Hz, 1H, Ph), 7.74 (t, *J* = 7.3, 14.7 Hz, 1H, Ph), 7.98 (d, *J* = 7.9, 15.3 Hz, 1H, Ph), 8.06 (s, 1H, F-5), 8.12 (d, *J* = 8.1 Hz, 1H, NH), 8.43 (d, *J* = 7.6 Hz, 1H, NH), 8.90ppm (d, *J* = 8.4 Hz, 1H, NH); ^{13}C NMR (100 MHz, DMSO-d6): δ = 21.9, 23.5, 24.8, 37.2, 37.7, 52.9, 54.3, 54.6, 55.3, 113.1, 113.9, 119.6, 124.4, 126.7, 128.5, 129.5, 129.6, 129.7, 130.6, 131.3, 132.3, 133.7, 138.2, 147.6, 148.7, 150.8, 158.2, 165.5, 170.9, 171.3, 187.5 ppm; HRMS (ESI) *m/z* $[M+H]^+$ calcd for $C_{36}H_{39}N_4O_8$: 655.2768, found: 655.2769; HPLC: t_R = 8.92 min (98.7% purity).

4.1.10 2-bromo-N-((S)-1-(((S)-1-(((S)-1-(furan-2-yl)-4-methyl-1-oxopentan-2-yl)amino)-3-(4-methoxyphenyl)-1-oxopropan-2-yl)amino)-1-oxo-3-phenylpropan-2-yl)benzamide (7j): Following the same procedure as described for the synthesis of **7a** except for starting from **6j**, **7j** was obtained in 84% yield as a white solid; mp: 183-185□; ^{1}H NMR (400 MHz, DMSO-d_6): δ = 0.91 (dd, *J* = 6.5, 11.3 Hz, 6H, CH_3), 1.45-1.60 (m, 2H, CH_2), 1.63-1.68 (m, 1H, CH), 2.70-2.82 (m, 2H, CH_2), 2.94 (dd, *J* = 5.0, 13.9 Hz, 1H, CH_2), 3.04(dd, *J* =3.9, 14.0 Hz, 1H, CH_2), 3.69 (s, 3H, OCH_3), 4.56-4.63 (m, 1H, CH), 4.64-4.71 (m, 1H, CH), 5.02-5.09 (m, 1H, CH), 6.75 (t, *J* = 1.9 Hz, 2H, Ph), 6.77 (s, 1H, F-4), 7.06 (dd, *J* = 1.8, 7.4 Hz, 1H, Ph), 7.12 (d, *J* = 8.6 Hz, 2H, Ph), 7.18-7.22 (m, 1H, Ph), 7.26-7.40 (m, 6H, Ph),7.49 (d, *J* = 3.5 Hz, 1H, F-3), 7.59 (d, *J* = 7.6 Hz, 1H, Ph), 8.01 (d, *J* = 8.2 Hz, 1H, NH), 8.05 (d, *J* = 1.04 Hz, 1H, F-5), 8.48 (d, *J* = 7.8 Hz, 1H, NH), 8.57 ppm (d, *J* = 8.5 Hz, 1H, NH); ^{13}C NMR (100 MHz, DMSO-d6): δ = 21.9, 23.5, 24.8,

37.4, 37.7, 52.9, 54.2, 54.7,55.4, 113.1, 113.9, 119.3, 119.6, 126.7, 127.8, 128.5, 129.2, 129.6, 129.7, 130.7, 131.4, 133.1, 138.3, 139.0, 148.7, 150.8, 158.3, 167.3, 171.0, 171.3, 187.5 ppm; HRMS (ESI) *m/z* $[M+H]^+$ calcd for $C_{36}H_{39}BrN_3O_6$: 688.2022, found: 688.2027; HPLC: t_R = 9.44 min (99.0% purity).

4.1.11 (S)-2-amino-N-((S)-1-(furan-2-yl)-4-methyl-1-oxopentan-2-yl)propanamide hydrochloride (8a): EDC·HCl (230 mg, 1.2 mmol) and HOBt (162 mg, 1.2 mmol) were added to a solution of Boc-Ala-OH (189 mg, 1 mmol), and **3** (217 mg, 1 mmol) in the presence of NMM (0.34 mL,3 mmol) in 10 mL DMF. The reaction mixture was stirred at room temperature overnight and diluted with EtOAc and washed with10% citric acid, saturated aqueous $NaHCO_3$ and brine, dried with Na_2SO_4, and concentrated in vacuo to give the crude product, which was separated by silica gel chromatography to yield Boc-Ala-Leu-Furan as a white solid (265 mg, 75%); mp: 118-119□; ^{1}H NMR (400 MHz, $CDCl_3$): δ = 0.91 (d, *J* = 6.4 Hz, 3H, CH_3), 1.03 (d, *J* = 6.2 Hz, 3H, CH_3), 1.35 (d, *J* = 7.0 Hz, CH_3), 1.45 (s, 9H, Boc), 1.52-1.57 (m, 1H,CH), 1.61-1.72 (m, 2H, CH_2), 4.19 (s, 1H, CH), 5.01 (s, 1H, CH), 5.36-5.42 (m, 1H, NH), 6.57 (dd, *J* = 1.6, 3.5 Hz, 1H, F-4), 6.69 (d, *J* = 8.1 Hz, 1H, NH), 7.34 (d, *J* = 3.5 Hz, 1H, F-3), 7.64 ppm (d, *J* = 0.8 Hz, 1H, F-5); ^{13}C NMR (100 MHz, $CDCl_3$): δ = 18.4, 21.7, 23.1, 24.8, 28.2, 41.5, 49.8, 52.5, 79.5, 112.5, 119.0, 147.2, 150.8, 155.3, 172.8, 187.6 ppm; HRMS (ESI) *m/z* $[M+H]^+$ calcd for $C_{18}H_{29}N_2O_5$: 353.20710, found: 353.20737. To a solution of Boc-Ala-Leu-Furan (265 mg, 0.75 mmol) in CH_2Cl_2 (0.75 mL), 4N HCl in 1, 4-dioxane (2.25 mL) was added. After 1 h, Et_2O (9 mL) was added. The reaction mixture was filtered, and then the precipitate was rinsed with enough Et_2O and dried. The crude product **8a** was used for the next step without further purification.

4.1.12 (S)-2-amino-N-((S)-1-(furan-2-yl)-4-methyl-1-oxopentan-2-yl)-3-methoxypropanamide hydrochloride (8b): Following the same procedure as described for the synthesis of **8a** except for starting from Boc-Ser(OMe)-OH, Boc-Ser(OMe)-Leu-Furan was obtained in 75% yield as a white solid; mp: 80-82□; ^{1}H NMR (400MHz, DMSO-d_6): δ = 0.90 (t, *J* = 6.0, 6,4 Hz, 6H, CH_3), 1.38 (s, 9H,CH_3), 1.48-1.59 (m, 2H, CH_2), 1.66-1.69 (m, 1H, CH), 3.19 (s, 3H, OCH_3), 3.39-3.46 (m, 2H, CH_2), 4.16-4.21 (m, 1H, CH), 5.00-5.05 (m, 1H, CH), 6.73 (dd, *J* = 1.4, 3.4 Hz, 1H, F-4), 6.86 (d, *J* = 8.2 Hz, 1H, NH), 7.47 (d, *J* = 3.6 Hz, 1H, F-3), 8.03 (s, 1H, F-5), 8.28 ppm (d, *J* = 7.7 Hz, 1H, NH); ^{13}C NMR (100 MHz, DMSO-d_6): δ =21.8, 23.6, 24.7, 28.6, 53.0, 54.6, 58.5, 72.3, 78.7, 113.1, 119.5, 148.6, 150.7, 155.6, 170.4, 187.6 ppm;

HRMS (ESI) *m/z* $[M+H]^+$ calcd for $C_{19}H_{31}N_2O_6$: 383.21766, found: 383.21799. To a solution of Boc-Ser(OMe)-Leu-Furan (287 mg, 0.75 mmol) in CH_2Cl_2 (0.75 mL), 4N HCl in 1,4-dioxane (2.25 mL) was added. After1 h, Et_2O (9 mL) was added. The reaction mixture was filtered, and then the precipitate was rinsed with enough Et_2O and dried. The crude product **8b** was used for the next step without further purification.

4.1.13 (S)-2-amino-N-((S)-1-(furan-2-yl)-4-methyl-1-oxopentan-2-yl)-3-(4-hydroxyphenyl)propanamide hydrochloride (8c): Following the same procedure as described for the synthesis of **8a** except for starting from Boc-Tyr-OH, Boc-Tyr-Leu-Furan was obtained in 63% yield as a white solid; mp: 76-78□; ^{1}H NMR (400 MHz, DMSO-d_6): δ = 0.90-0.92 (m, 6H, CH_3), 1.31 (s, 9H, Boc), 1.48-1.61 (m, 2H, CH_2), 1.69-1.71 (m, 1H, CH), 2.54-2.80 (m, 2H, CH_2Ph), 4.04-4.13 (m, 1H, CH), 5.03-5.08 (m, 1H, CH), 6.61 (d, *J* = 8.1 Hz, 2H, Ph), 6.74 (s, 1H, F-4), 6.81 (d, *J* = 8.5 Hz, 1H, NH), 7.01 (d, *J* = 8.1 Hz, 2H, Ph), 7.47 (d, *J* = 3.3Hz, 1H, F-3), 8.04 (s, 1H, F-5), 8.26 (d, *J* = 7.7 Hz, 1H, NH), 9.14 ppm (s, 1H, OH); ^{13}C NMR (100 MHz, DMSO-d_6): δ = 21.8, 23.6, 24.7, 28.6, 36.9, 52.8, 56.3, 78.4, 113.1, 115.2, 119.5, 128.5, 130.5, 148.6, 150.8, 155.6, 156.2, 172.4, 187.8 ppm; HRMS (ESI) *m/z* $[M+H]^+$ calcd for $C_{24}H_{33}N_2O_6$: 445.23331, found: 445.23358. To a solution of Boc-Tyr-Leu-Furan (280 mg, 0.63 mmol) in CH_2Cl_2 (0.63 mL), 4N HCl in 1,4-dioxane (1.89 mL) was added. After 1 h, Et_2O (8 mL) was added. The reaction mixture was filtered, and then the precipitate was rinsed with enough Et_2O and dried. The crude product **8c** was used for the next step without further purification.

4.1.14 (S)-2-amino-4-(isopentylamino)-4-oxobutanoic acid hydrochloride (9a): EDC·HCl (230 mg, 1.2 mmol) and HOBt (162 mg, 1.2 mmol) were added to a solution of Boc-Asp-O*t*Bu (289 mg, 1 mmol), and isoamylamine (87 mg, 1 mmol) in the presence of NMM (0.34 mL,3 mmol) in 10 mL DMF. The reaction mixture was stirred at room temperature overnight and diluted with EtOAc and washed with10% citric acid, saturated aqueous $NaHCO_3$ and brine, dried withNa_2SO_4, and concentrated in vacuo to give the crude product, which was separated by silica gel chromatography to yield Boc-IsoamylAsn-O*t*Bu as a white solid (313 mg, 87%); mp: 107-108□; ^{1}H NMR (400 MHz, $CDCl_3$): δ = 0.90 (s, 3H, CH_3), 0.91 (s, 3H, CH_3), 1.38 (dd, *J* = 7.1, 14.8 Hz, 2H, CH_2), 1.44 (s, 9H, CH_3), 1.46 (s, 9H, CH_3), 1.59-1.64 (m, 1H, CH), 2.65 (dd, *J* = 3.8, 15.0 Hz, 1H, CH_2), 2.76 (dd, *J* = 4.9, 15.6 Hz, 1H, CH_2), 3.25 (dd, *J* = 6.8, 13.6 Hz, 2H, NCH_2), 4.35 (t, *J* = 4.3, 7.2 Hz, 1H, CH), 5.66 ppm (s,2H, NH); MS (ESI) *m/z*(%): 359.3 (100) $[M+H]^+$. To a solution of Boc-IsoamylAsn-O*t*Bu (313 mg, 0.87 mmol) in CH_2Cl_2 (0.87 mL), 4N

HCl in 1,4-dioxane (2.61 mL) was added. After 1 h, Et_2O (10 mL) was added. The reaction mixture was filtered, and then the precipitate was rinsed with enough Et_2O and dried. The crude product **9a** was used for the next step without further purification.

4.1.15 (S)-2-amino-4-(isobutylamino)-4-oxobutanoic acid hydrochloride (9b): Following the same procedure as described for the synthesis of **9a** except for starting from isobutylamine, Boc-IsobutylAsn-O*t*Bu was obtained in 93% yield as a white solid; mp: 142□; ^{1}H NMR (400 MHz, $CDCl_3$): δ = 0.89 (s, 3H, CH_3), 0.91 (s, 3H, CH_3), 1.44 (s, 9H, CH_3), 1.46 (s, 9H, CH_3), 1.70-1.80 (m, 1H, CH), 2.68 (dd, *J* = 3.8, 15.6 Hz, 1H, CH_2), 2.80 (dd, *J* = 4.1, 16.1 Hz, 1H, CH_2), 3.06 (t, *J* = 6.5, 12.8 Hz, 2H, NCH_2), 4.35 (t, *J* = 4.3, 7.3 Hz, 1H, CH), 5.72 ppm (s, 2H, NH); MS (ESI) *m/z* (%): 345.2 (100) $[M+H]^+$. To a solution of Boc-IsobutylAsn-O*t*Bu (1 mmol) in CH_2Cl_2 (1 mL), 4N HCl in 1,4-dioxane (3 mL) was added. After1 h, Et_2O (12 mL) was added. The reaction mixture was filtered, and then the precipitate was rinsed with enough Et_2O and dried. The crude product **9b** was used for the next step without further purification.

4.1.16 (S)-2-amino-4-(neopentylamino)-4-oxobutanoic acid hydrochloride (9c): Following the same procedure as described for the synthesis of **9a** except for starting from neopentylamine, Boc-NeopentylAsn-O*t*Bu was obtained in 97% yield as a white solid; mp: 115□; ^{1}H NMR (400 MHz, $CDCl_3$): δ = 0.82 (s, 9H, CH_3), 1.37 (s, 18H, CH_3), 2.43-2.56 (m, 2H, CH_2), 2.80 (dd, *J* = 5.9, 13.1 Hz, 1H, CH_2), 2.92 (dd, *J* = 6.6, 13.1 Hz, 1H, CH_2), 4.17 (dd, *J* = 7.7, 13.6 Hz, 1H, CH), 6.93 (d, *J* = 8.2 Hz, 1H, CH_2), 7.73 ppm (t, *J* = 6.1, 12.2 Hz, 1H, CH); MS (ESI) *m/z* (%): 381.5 (100) $[M+Na]^+$. To a solution of Boc-NeopentylAsn-O*t*Bu (1 mmol) in CH_2Cl_2 (1 mL), 4N HCl in 1,4-dioxane (3 mL) was added. After 1 h, Et_2O (12 mL) was added. The reaction mixture was filtered, and then the precipitate was rinsed with enough Et_2O and dried. The crude product 9c was used for the next step without further purification.

4.1.17 (S)-4-(isopentylamino)-2-(4-methylphenylsulfonamido)-4-oxobutanoic acid (10a):

Compound **9a** (2.38 g, 10 mmol) was dissolved in THF (24 mL) and 1 N NaOH (12 mL), and then cooled in ice bath. *p*-Toluenesulfonyl chloride (1.90 g, 10 mmol) was added portionwise to the vigorously stirred solution. The pH of the reaction mixture was frequently adjusted to >8 with 4 N NaOH. After 2 h, the mixture was acidified with 6 M HCl and then extracted thrice with EtOAc. The combined organic phase was washed with 1 M HCl, water, and brine, dried with Na_2SO4, and concentrated in vacuo to give **10a** (3.07 g, 84%) as a white solid.

4.1.18 (S)-4-(isobutylamino)-2-(4-methylphenylsulfonamido)-4-oxobutanoic acid (10b): Following the same procedure as described for the synthesis of **10a** except for starting from **9b**, **10b** was obtained in 85% yield as a white solid.

4.1.19 (S)-2-(4-methylphenylsulfonamido)-4-(neopentylamino)-4-oxobutanoic acid (10c): Following the same procedure as described for the synthesis of **10a** except for starting from **9c**, **10c** was obtained in 75% yield as a white solid.

4.1.20 (S)-2-(4-methylphenylsulfonamido)-3-phenylpropanoic acid (10d): Following the same procedure as described for the synthesis of **10a** except for starting from H-Phe-OH, **10d** was obtained in 90% yield as a white solid.

4.1.21 (S)-3-(4-methoxyphenyl)-2-(4-methylphenylsulfonamido)propanoic acid (10e): Following the same procedure as described for the synthesis of **10a** except for starting from H-(4-OMe)Phe-OH, **10e** was obtained in 90% yield as a white solid.

4.1.22 (S)-2-acetamido-N-((S)-1-(((S)-1-(furan-2-yl)-4-methyl-1-oxopentan-2-yl)amino)-3-(4-hydroxyphenyl)-1-oxopropan-2-yl)-3-phenylpropanamide (11a): EDC·HCl (230 mg, 1.2 mmol) and HOBt (162 mg, 1.2 mmol) were added to a solution of Ac-Phe-OH (207 mg, 1 mmol), and **8c** (380 mg, 1 mmol) in the presence of NMM (0.34 mL, 3 mmol) in 10 mL DMF. The reaction mixture was stirred at room temperature overnight and diluted with EtOAc and washed with10% citric acid, saturated aqueous $NaHCO_3$ and brine, dried with Na_2SO_4, and concentrated in vacuo to give the crude product, which was separated by silica gel chromatography to yield **11a** as a white solid (399 mg, 75%); mp: 197-199□; ^{1}H NMR (400 MHz, DMSO-d_6): δ = 0.90 (d, J = 6.8 Hz, 3H, CH_3), 0.92 (d, J = 6.7 Hz, 3H, CH_3), 1.48-1.57 (m, 2H, CH_2), 1.66-1.67 (m, 1H, CH), 1.72 (s, 3H, CH_3), 2.62-2.68 (m, 2H, CH_2), 2.85-2.95 (m, 2H, CH_2), 4.43-4.49 (m, 2H, CH), 5.01-5.06 (m, 1H, CH), 6.60 (d, J = 8.4 Hz, 2H, Ph), 6.73 (q, J = 1.6, 3.5 Hz, 1H, F-4), 6.98 (d, J = 8.4 Hz, 2H, Ph), 7.16-7.23 (m, 5H, Ph), 7.47 (d, J = 3.5 Hz, 1H, F-3), 8.02 (m, 3H, NH, F-5), 8.35 (d, J = 7.7 Hz, 1H, NH), 9.15 ppm (s, 1H, OH); ^{13}C NMR (100 MHz, DMSO-d_6): δ = 21.9, 22.9, 23.5, 24.8, 37.1, 37.8, 52.9, 54.2, 54.4, 113.1, 115.3, 119.5, 126.6, 128.0, 128.4, 129.6, 130.6, 138.5, 148.7, 150.8, 156.3, 169.5, 171.5, 171.6, 187.6 ppm; HRMS (ESI) m/z $[M+H]^+$ calcd for $C_{30}H_{36}N_3O_6$: 534.25986, found: 534.25893; HPLC: t_R = 8.60 min (98.8% purity).

4.1.23 (S)-N-((S)-1-(furan-2-yl)-4-methyl-1-oxopentan-2-yl)-3-(4-hydroxyphenyl)-2-((S)-2-(4-methylphenylsulfonamido)-3-phenylpropanamido)propanamide (11b):

Following the same procedure as described for the synthesis of **11a** except for starting from **10d** and **8c**, **11b** was obtained in 81% yield as a white solid; mp: 227-229□; ^{1}H NMR (400 MHz, DMSO-d_6): δ = 0.88 (d, J = 6.8 Hz, 3H, CH_3), 0.89 (d, J = 6.7 Hz, 3H, CH_3), 1.43-1.53 (m, 2H, CH_2), 1.61-1.66 (m, 1H, CH), 2.29 (s, 3H, CH_3), 2.54-2.58 (m, 2H, CH_2), 2.74-2.82 (m, 2H, CH_2), 3.95-4.01 (m, 1H, CH), 4.23-4.29 (m, 1H, CH), 4.97-5.03 (m, 1H, CH), 6.63 (d, J = 8.4 Hz, 2H, Ph), 6.71 (dd, J = 1.6, 3.6 Hz, 1H, F-4), 6.96 (d, J = 8.4 Hz, 2H, Ph), 7.05 (d, J = 8.2 Hz, 2H, Ph), 7.10-7.18 (m, 5H, Ph), 7.30 (d, J = 8.2 Hz, 2H, Ph), 7.45 (d, J = 3.6 Hz, 1H, F-3), 7.89 (d, J = 9.1 Hz, 1H, NH), 8.03 (d, J = 1.1 Hz, 1H, F-5), 8.16 (d, J = 8.0 Hz, 1H, NH), 8.34 (d, J = 7.7 Hz, 1H, NH), 9.19 ppm (s, 1H, OH); ^{13}C NMR (100 MHz, DMSO-d_6): δ = 21.4, 21.9, 23.5, 24.8, 37.0, 38.8, 52.9, 54.4, 57.9, 113.1, 115.3, 119.5, 126.6, 126.7, 128.0, 128.4, 129.5, 129.7, 130.6, 137.7, 138.5, 142.4, 148.6, 150.8, 156.3, 170.8, 171.4, 187.5 ppm; HRMS (ESI) *m/z* $[M+H]^+$ calcd for $C_{35}H_{40}N_3O_7S$: 646.25815, found: 646.25615; HPLC: t_R = 8.51 min (98.2% purity).

4.1.24 (S)-N-((S)-1-(furan-2-yl)-4-methyl-1-oxopentan-2-yl)-3-(4-hydroxyphenyl)-2-((S)-3-(4-methoxyphenyl)-2-(4-methylphenylsulfonamido)propanamido)propanamide (11c):

Following the same procedure as described for the synthesis of **11a** except for starting from **10e** and **8c**, **11c** was obtained in 82% yield as a white solid; mp: 174-175□; ^{1}H NMR (400 MHz, DMSO-d_6): δ = 0.89 (t, J = 6.9 Hz, 6H, CH_3), 1.42-1.57 (m, 2H, CH_2), 1.61-1.67 (m, 1H, CH), 2.29 (s, 3H, CH_3), 2.44-2.48 (m, 1H, CH_2), 2.53-2.58 (m, 1H, CH_2), 2.70-2.81(m, 2H, CH_2), 3.72 (s, 3H, OCH_3), 3.86-3.93 (m, 1H, CH), 4.26-4.32 (m, 1H, CH), 4.97-5.04 (m, 1H, CH), 6.62 (d,J = 8.4 Hz, 2H, Ph), 6.69 (s, 1H, F-4), 6.71-6.73 (m, 2H, Ph), 6.94-7.06 (m, 4H, Ph), 7.30 (d, J = 8.2 Hz, 2H, Ph), 7.45 (d, J = 3.5 Hz, 1H, F-3), 7.84 (d, J = 9.0 Hz, 1H, NH), 8.02 (d, J = 1.0 Hz, 1H, F-5), 8.12 (d, J = 8.0 Hz, 1H, NH), 8.33 (d, J = 7.7 Hz, 1H, NH), 9.17 ppm (s, 1H, OH); ^{13}C NMR (100 MHz, DMSO-d_6): δ = 21.4, 21.9, 23.5, 24.8, 37.1, 38.0, 52.9, 54.4, 55.3, 58.3, 113.1, 113.7, 115.3, 119.5, 126.7, 127.9, 129.4, 129.5, 130.6, 130.7, 138.5, 142.3, 148.6, 150.8, 156.3, 158.2, 170.9, 171.3, 187.5 ppm; HRMS (ESI) *m/z* $[M+H]^+$ calcd for $C_{36}H_{42}N_3O_8S$: 676.2674, found: 676.2684; HPLC: t_R = 8.42 min (100% purity).

4.1.25 tert-butyl-((S)-1-(((S)-1-(((S)-1-(furan-2-yl)-4-methyl-1-oxopentan-2-yl)amino)-1-oxopropan-2-yl)amino)-1-oxo-3-phenylpropan-2-yl)carbamate (11d):

Following the same procedure as described for the synthesis of **11a** except for starting from Boc-Phe-OH and **8a**, **11d** was obtained in 81% yield as a white solid; mp: 97-98□; ^{1}H NMR (400 MHz, DMSO-d_6): δ = 0.89 (d, J = 7.5 Hz, 3H, CH_3), 0.92 (d, J = 7.2 Hz, 3H, CH_3), 1.18 (d, J =

6.9 Hz, 3H, CH_3), 1.29 (s, 9H, Boc), 1.44-1.57 (m, 2H, CH_2), 1.66-1.69 (m, 1H, CH), 2.66-2.99 (m, 2H, CH_2), 4.12-4.17 (m, 1H, CH), 4.33-4.37 (m, 1H, CH), 4.99-5.05 (m, 1H, CH), 6.74 (t, *J* = 1.5, 3.5 Hz, 1H, F-4), 6.94 (d, *J* = 8.5 Hz, 1H, NH), 7.18-7.26 (m, 5H, Ph), 7.47 (d, *J* = 3.5 Hz, 1H, F-3), 7.99 (d, *J* = 7.3 Hz, 1H, NH), 8.04 (s, 1H, F-5), 8.35 ppm (d, *J* = 7.6 Hz, 1H, NH); ^{13}C NMR (100 MHz, DMSO-d_6): δ = 18.8, 21.8, 23.5, 24.9, 28.6, 37.7, 48.2, 53.0, 56.1, 78.5, 113.1, 119.3, 126.6, 128.4, 129.6, 138.7, 148.6, 150.8, 155.7, 171.8, 172.6, 187.8 ppm; HRMS (ESI) *m/z* $[M+H]^+$ calcd for $C_{27}H_{38}N_3O_6$: 500.27551, found: 500.27585; HPLC: t_R = 8.52 min (99.2% purity).

4.1.26 benzyl-((S)-1-(((S)-1-(((S)-1-(furan-2-yl)-4-methyl-1-oxopentan-2-yl)amino)-1-oxopropan-2-yl)amino)-1-oxo-3-phenylpropan-2-yl)carbamate (11e):

Following the same procedure as described for the synthesis of **11a** except for starting from Cbz-Phe-OH and **8a**, **11e** was obtained in 81% yield as a white solid; mp: 190-191□; ^{1}H NMR (400 MHz, DMSO-d_6): δ = 0.90 (d, *J* = 7.1 Hz, 3H, CH_3), 0.92 (d, *J* = 7.2 Hz, 3H, CH_3), 1.20 (d, *J* = 7.0 Hz, 3H, CH_3), 1.46-1.59 (m, 2H, CH_2), 1.67-1.72 (m, 1H, CH), 2.70-3.03 (m, 2H, CH_2), 4.24-4.30 (m, 1H, CH), 4.33-4.37 (m, 1H, CH), 4.93 (s, 2H, CH_2), 5.00-5.04 (m, 1H, CH), 6.74 (dd, *J* = 1.6, 3.6 Hz, 1H, F-4), 7.19-7.34 (m, 10H, Ph), 7.48 (d, *J* = 3.2 Hz, 1H, F-3), 7.50 (s, 1H, NH), 8.04 (d, *J* = 1.0 Hz, 1H, F-5), 8.17 (d, *J* = 7.4 Hz, 1H, NH), 8.33 ppm (d, *J* = 7.5 Hz, 1H, NH); ^{13}C NMR (100 MHz, DMSO-d_6): δ = 18.6, 21.9, 23.5, 24.9, 37.8, 48.4, 53.1, 56.5, 65.6, 113.1, 119.3, 126.7, 127.8, 128.1, 128.5, 128.7, 129.7, 137.5, 138.6, 148.6, 150.8, 156.3, 171.6, 172.6, 187.8 ppm; HRMS (ESI) *m/z* $[M+H]^+$ calcd for $C_{30}H_{36}N_3O_6$: 534.25986, found: 534.25955; HPLC: t_R = 8.70 min (99.6% purity).

4.1.27 tert-butyl-((S)-1-(((S)-1-(((S)-1-(furan-2-yl)-4-methyl-1-oxopentan-2-yl)amino)-1-oxopropan-2-yl)amino)-3-(4-methoxyphenyl)-1-oxopropan-2-yl)carbamate (11f):

Following the same procedure as described for the synthesis of **11a** except for starting from **4a** and **8a**, **11f** was obtained in 73% yield as a white solid; mp: 97-99□; ^{1}H NMR (400 MHz, DMSO-d_6): δ = 0.89 (d, *J* = 7.3 Hz, 3H, CH_3), 0.92 (d, *J* = 7.4 Hz, 3H, CH_3), 1.18 (d, *J* = 6.9 Hz, 3H, CH_3), 1.29 (s, 9H, Boc), 1.44-1.57 (m, 2H, CH_2), 1.65-1.68 (m, 1H, CH), 2.59-2.91 (m, 2H, CH_2), 3.71 (s, 3H, OCH_3), 4.04-4.10 (m, 1H, CH), 4.31-4.37 (m, 1H, CH), 4.99-5.05 (m, 1H, CH), 6.74 (dd, *J* = 1.5, 4.9 Hz, 1H, F-4), 6.82 (d, *J* = 8.3 Hz, 2H, Ph), 6.88 (d, *J* = 8.5 Hz, 1H, NH), 7.17 (d, *J* = 8.3 Hz, 2H, Ph), 7.47 (d, *J* = 3.5 Hz, 1H, F-3), 7.97 (d, *J* = 7.4 Hz, 1H, NH), 8.04 (s, 1H, F-5), 8.34 ppm (d, *J* = 7.6 Hz, 1H, NH); ^{13}C NMR (100 MHz, DMSO-d_6): δ = 18.8,

21.8, 23.5, 24.9, 28.6, 36.9, 48.2, 53.0, 55.4, 56.4, 78.5, 113.1, 113.9, 119.3, 130.5, 130.6, 148.6, 150.8, 155.7, 158.2, 171.8, 172.6, 187.8 ppm; HRMS (ESI) *m/z* $[M+H]^+$ calcd for $C_{28}H_{40}N_3O_7$: 530.28608, found: 530.28602; HPLC: t_R = 8.35 min (98.5% purity).

4.1.28 tert-butyl-((S)-1-(((S)-1-(((S)-1-(furan-2-yl)-4-methyl-1-oxopentan-2-yl)amino)-3-methoxy-1-oxopropan-2-yl)amino)-1-oxo-3-phenylpropan-2-yl)carbamate (11g):

Following the same procedure as described for the synthesis of **11a** except for starting from Boc-Phe-OH and **8b**, **11g** was obtained in 80% yield as a white solid; mp: 104-105□; ^{1}H NMR (400 MHz, DMSO-d_6): δ = 0.89 (d, *J* = 6.9 Hz, 3H, CH_3), 0.92 (d, *J* = 7.0 Hz, 3H, CH_3), 1.29 (s, 9H, Boc), 1.45-1.58 (m, 2H, CH_2), 1.64-1.69 (m, 1H, CH), 2.66-2.97 (m, 2H, CH_2), 3.21 (s, 3H, OCH_3), 3.47 (d, *J* = 5.6 Hz, 2H, CH_2), 4.17-4.22 (m, 1H, CH), 4.52-4.55 (m, 1H, CH), 5.01-5.07 (m, 1H, CH), 6.73 (dd, *J* = 1.7, 3.6 Hz, 1H, F-4), 6.94 (d, *J* = 8.5 Hz, 1H, NH), 7.18-7.27 (m, 5H, Ph), 7.47 (d, *J* = 3.4 Hz, 1H, F-3), 8.03 (d, *J* = 1.1 Hz, 1H, F-5), 8.05 (s, 1H, NH), 8.41 ppm (d, *J* = 7.8 Hz, 1H, NH); ^{13}C NMR (100 MHz, DMSO-d_6): δ = 21.9, 23.5, 24.8, 28.6, 37.7, 52.8, 53.0, 56.1, 58.7, 72.5, 78.5, 113.1, 119.5, 126.6, 128.4, 129.7, 138.7, 148.6, 150.7, 155.7, 169.8, 172.1, 187.5 ppm; HRMS (ESI) *m/z* $[M+H]^+$ calcd for $C_{28}H_{40}N_3O_7$: 530.28608, found: 530.28656; HPLC: t_R = 8.79 min (99.5% purity).

4.1.29 Benzyl-((S)-1-(((S)-1-(((S)-1-(furan-2-yl)-4-methyl-1-oxopentan-2-yl)amino)-3-methoxy-1-oxopropan-2-yl)amino)-1-oxo-3-phenylpropan-2-yl)carbamate (11h):

Following the same procedure as described for the synthesis of **11a** except for starting from Cbz-Phe-OH and **8b**, **11h** was obtained in 73% yield as a white solid; mp: 113□; ^{1}H NMR (400 MHz, DMSO-d_6): δ = 0.89 (d, *J* = 7.0 Hz, 3H, CH_3), 0.92 (d, *J* = 6.8 Hz, 3H, CH_3), 1.49-1.55 (m, 2H, CH_2), 1.67-1.68 (m, 1H, CH), 2.67-3.03 (m, 2H, CH_2), 3.22 (s, 3H, OCH_3), 3.49 (d, *J* = 5.6 Hz, 2H, CH_2), 4.30-4.36 (m, 1H, CH), 4.61-4.66 (m, 1H, CH), 4.93 (s, 2H, CH_2), 5.01-5.07 (m, 1H, CH), 6.73 (dd, *J* = 1.6, 3.5 Hz, 1H, F-4), 7.18-7.34 (m, 10H, Ph), 7.48 (d, *J* = 3.4 Hz, 1H, F-3), 7.51 (s, 1H, NH), 8.03 (d, *J* = 0.9 Hz, 1H, F-5), 8.23 (d, *J* = 7.8 Hz, 1H, NH), 8.38 ppm (d, *J* = 7.6 Hz, 1H, NH); ^{13}C NMR (100 MHz, DMSO-d_6): δ = 21.9, 23.5, 24.8, 37.9, 53.0, 53.1, 56.4, 58.7, 65.6, 72.4, 113.1, 119.5, 126.7, 127.8, 128.1, 128.4, 128.7, 129.7, 137.5, 138.6, 148.6, 150.7, 156.3, 169.8, 172.1, 187.5 ppm; HRMS (ESI) *m/z* $[M+H]^+$ calcd for $C_{31}H_{38}N_3O_7$: 564.27043, found: 564.26897; HPLC: t_R = 8.91 min (100% purity).

4.1.30 tert-butyl-((S)-1-(((S)-1-(((S)-1-(furan-2-yl)-4-methyl-1-oxopentan-2-yl)amino)-3-methoxy-1-oxopropan-2-yl)amino)-3-(4-methoxyphenyl)-1-oxopropan-2-yl)carbamate (11i):

Following the same procedure as described for the synthesis of **11a** except for starting from **4a** and **8b**, **11i** was obtained in 70% yield as a white solid; mp: 75-76□; ^{1}H NMR (400 MHz, DMSO-d_6): δ = 0.89 (d, J = 7.1 Hz, 3H, CH_3), 0.92 (d, J = 7.1 Hz, 3H, CH_3), 1.30 (s, 9H, Boc), 1.46-1.58 (m, 2H, CH_2), 1.64-1.67 (m, 1H, CH), 2.59-2.93 (m, 2H, CH_2), 3.21 (s, 3H, OCH_3), 3.46 (d, J = 5.4 Hz, 2H, CH_2), 3.71 (s, 3H, OCH_3), 4.10-4.15 (m, 1H, CH), 4.50-4.55 (m, 1H, CH), 5.01-5.07 (m, 1H, CH), 6.74 (dd, J = 1.3, 3.3 Hz, 1H, F-4), 6.82 (d, J = 8.2 Hz, 2H, Ph), 6.90 (d, J = 8.6 Hz, 1H, NH), 7.18 (d, J = 8.4 Hz, 2H, Ph), 7.48 (d, J = 3.5 Hz, 1H, F-3), 8.04 (s, 1H, F-5), 8.06 (s, 1H, NH), 8.42 ppm (d, J = 7.7 Hz, 1H, NH); ^{13}C NMR (100 MHz, DMSO-d_6): δ = 21.9, 23.5, 24.8, 28.6, 36.9, 52.8, 53.0, 55.4, 56.4, 58.7, 72.5, 78.5, 113.1, 113.9, 119.5, 130.5, 130.7, 148.7, 150.7, 155.7, 158.2, 169.9, 172.2, 187.5 ppm; HRMS (ESI) *m/z* $[M+H]^+$ calcd for $C_{29}H_{42}N_3O_8$: 560.29664, found: 560.29613; HPLC: t_R = 7.88 min (99.0% purity).

4.1.31 (S)-N1-((S)-1-(((S)-1-(furan-2-yl)-4-methyl-1-oxopentan-2-yl)amino)-1-oxopropan-2-yl)-2-(4-methylphenylsulfonamido)-N4-neopentylsuccinamide (11j):

Following the same procedure as described for the synthesis of **11a** except for starting from **10c** and **8a**, **11j** was obtained in 79% yield as a white solid; mp: 209-210□; ^{1}H NMR (400 MHz, DMSO-d_6): δ = 0.79 (s, 9H, CH_3), 0.88 (d, J = 3.5 Hz, 3H, CH_3), 0.89 (d, J = 3.5 Hz, 3H, CH_3), 1.00 (d, J = 7.1 Hz, 3H, CH_3), 1.43-1.49 (m, 1H, CH), 1.59-1.68 (m, 2H, CH_2), 2.23-2.55 (m, 2H, CH_2), 2.36 (s, 3H, CH_3), 2.75-2.86 (m, 2H, CH_2), 3.92-3.96 (m, 1H, CH), 4.04-4.09 (m, 1H, CH), 4.83-4.89 (m, 1H, CH), 6.69 (dd, J = 1.6, 3.6 Hz, 1H, F-4), 7.32 (d, J = 8.2 Hz, 2H, Ph), 7.41 (d, J = 3.5 Hz, 1H, F-3), 7.65 (d, J = 8.2 Hz, 2H, Ph), 7.79 (t, J = 6.0, 12.0 Hz, 1H, NH), 7.97 (s, 1H, NH), 7.99 (d, J = 1.2 Hz, 1H, F-5), 8.09 (d, J = 7.6 Hz, 1H, NH), 8.22 ppm (d, J = 7.3 Hz, 1H, NH); ^{13}C NMR (100 MHz, DMSO-d_6): δ = 18.0, 21.4, 21.9, 23.4, 24.8, 27.6, 32.2, 38.9, 48.3, 50.2, 53.5, 112.9, 119.2, 127.1, 129.7, 138.7, 142.9, 148.4, 150.7, 169.6, 170.0, 172.4, 187.7 ppm; HRMS (ESI) *m/z* $[M+H]^+$ calcd for $C_{29}H_{43}N_4O_7S$: 591.28470, found: 591.28308; HPLC: t_R = 8.15 min (99.0% purity).

4.1.32 (S)-N1-((S)-1-(((S)-1-(furan-2-yl)-4-methyl-1-oxopentan-2-yl)amino)-1-oxopropan-2-yl)-N4-isopentyl-2-(4-methylphenylsulfonamido)succinamide (11k):

Following the same procedure as described for the synthesis of **11a** except for starting from **10a** and **8a**, **11k** was obtained in 81% yield as a white solid; mp: 210□; ^{1}H NMR (400 MHz, DMSO-d_6): δ = 0.81 (d, J = 6.5 Hz, 6H, CH_3), 0.88 (d, J = 6.2 Hz, 6H, CH_3), 1.01 (d, J = 7.1 Hz, 3H, CH_3), 1.19-1.25 (m, 2H, CH_2), 1.41-1.54 (m, 2H, CH_2), 1.61-1.73 (m, 2H, CH), 2.23-2.47 (m,

2H, CH_2), 2.36 (s, 3H, CH_3), 2.95-2.97 (m, 2H, CH_2), 3.93-3.97 (m, 1H, CH), 4.03-4.08 (m, 1H, CH), 4.84-4.89 (m, 1H, CH), 6.69 (dd, *J* = 1.6, 3.4 Hz, 1H, F-4), 7.32 (d, *J* = 8.1 Hz, 2H, Ph), 7.41 (d, *J* = 3.6 Hz, 1H, F-3), 7.65 (d, *J* = 8.2 Hz, 2H, Ph), 7.86 (t, *J* = 5.3, 10.6 Hz, 1H, NH), 7.97 (s, 1H, NH), 7.99 (s, 1H, F-5), 8.13 (d, *J* = 7.6 Hz, 1H, NH), 8.21 ppm (d, *J* = 7.4 Hz, 1H, NH); ^{13}C NMR (100 MHz, DMSO-d_6): δ = 17.9, 21.4, 21.8, 22.7, 22.8, 23.4, 24.8, 25.6, 37.3, 38.2, 38.9, 48.3, 53.4, 53.5, 112.9, 119.2, 127.1, 129.7, 138.8, 142.9, 148.4, 150.7, 169.2, 170.0, 172.4, 187.7 ppm; HRMS (ESI) *m/z* $[M+H]^+$ calcd for $C_{29}H_{43}N_4O_7S$: 591.28470, found: 591.28302; HPLC: t_R = 8.26 min (98.1% purity).

4.1.33 (S)-N1-((S)-1-(((S)-1-(furan-2-yl)-4-methyl-1-oxopentan-2-yl)amino)-1-oxopropan-2-yl)-N4-isobutyl-2-(4-methylphenylsulfonamido)succinamide (11l): Following the same procedure as described for the synthesis of **11a** except for starting from **10b** and **8a**, **11l** was obtained in 79% yield as a white solid; mp: 233-234□; ^{1}H NMR (400 MHz, DMSO-d_6): δ = 0.77 (d, *J* = 3.5 Hz, 3H, CH_3), 0.78 (d, *J* = 3.5 Hz, 3H, CH_3), 0.88 (d, *J* = 1.4 Hz, 3H, CH_3), 0.89 (d, *J* = 1.3 Hz, 3H, CH_3), 1.01 (d, *J* = 7.1 Hz, 3H, CH_3), 1.42-1.48 (m, 1H, CH), 1.56-1.70 (m, 3H, CH, CH_2), 2.27-2.53 (m, 2H, CH_2), 2.36 (s, 3H, CH_3), 2.76-2.80 (m, 2H, CH_2), 3.95-3.97 (m, 1H, CH), 4.03-4.09 (m, 1H, CH), 4.84-4.89 (m, 1H, CH), 6.69 (dd, *J* = 1.6, 3.5 Hz, 1H, F-4), 7.32 (d, *J* = 8.1 Hz, 2H, Ph), 7.41 (d, *J* = 3.5 Hz, 1H, F-3), 7.65 (d, *J* = 8.2 Hz, 2H, Ph), 7.89 (t, *J* = 5.6, 11.3 Hz, 1H, NH), 7.96 (s, 1H, NH), 7.99 (d, *J* = 1.2 Hz, 1H, F-5), 8.09 (d, *J* = 7.6 Hz, 1H, NH), 8.22 ppm (d, *J* = 7.3 Hz, 1H, NH); ^{13}C NMR (100 MHz, DMSO-d_6): δ = 18.0, 20.5, 21.4, 21.8, 23.4, 24.8, 28.3, 38.9, 46.6, 48.3, 53.4, 53.5, 113.0, 119.2, 127.1, 129.7, 138.8, 142.9, 148.4, 150.7, 169.4, 170.0, 172.4, 187.7 ppm; HRMS (ESI) *m/z* $[M+H]^+$ calcd for $C_{28}H_{41}N_4O_7S$: 577.26905, found: 577.26793; HPLC: t_R = 7.62 min (98.3% purity).

4.1.34 (S)-N1-((S)-1-(((S)-1-(furan-2-yl)-4-methyl-1-oxopentan-2-yl)amino)-3-methoxy-1-oxopropan-2-yl)-2-(4-methylphenylsulfonamido)-N4-neopentylsuccinamide (11m):

Following the same procedure as described for the synthesis of **11a** except for starting from **10c** and **8b**, **11m** was obtained in 81% yield as a white solid; mp: 156-157□; ^{1}H NMR (400 MHz, DMSO-d_6): δ = 0.79 (s, 9H, CH_3), 0.87 (d, *J* = 3.7 Hz, 3H, CH_3), 0.89 (d, *J* = 3.7 Hz, 3H, CH_3), 1.43-1.49 (m, 1H, CH), 1.59-1.69 (m, 2H, CH_2), 2.30-2.50 (m, 2H, CH_2), 2.37 (s, 3H, CH_3), 2.80 (dd, *J* = 1.9, 6.1 Hz, 2H, CH_2), 3.17 (s, 3H, OCH_3), 3.27 (dd, *J* = 4.4, 9.7 Hz, 1H, CH_2), 3.44 (dd, *J* = 5.5, 9.8 Hz, 1H, CH_2), 4.14-4.22 (m, 2H, CH), 4.86-4.91 (m, 1H, CH), 6.69 (dd, *J* = 1.6, 3.6 Hz, 1H, F-4), 7.32 (d, *J* = 8.2 Hz, 2H, Ph), 7.43 (d, *J* = 3.6 Hz, 1H, F-3), 7.65 (d, *J* = 8.2 Hz, 2H,

Ph), 7.77 (t, *J* = 6.0, 12.2 Hz, 1H, NH), 7.95 (d, *J* = 8.8 Hz, 1H, NH), 7.99 (d, *J* = 1.2 Hz, 1H, F-5), 8.13 (d, *J* = 7.9 Hz, 1H, NH), 8.32 ppm (d, *J* = 7.5 Hz, 1H, NH); ^{13}C NMR (100 MHz, DMSO-d_6): δ = 21.4, 21.9, 23.4, 24.7, 27.7, 32.2, 39.0, 50.2, 53.1, 53.4, 53.6, 58.7, 72.0, 112.9, 119.4, 127.1, 129.8, 138.7, 142.9, 148.4, 150.6, 169.5, 169.8, 170.6, 187.5 ppm; HRMS (ESI) *m/z* $[M+H]^+$ calcd for $C_{30}H_{45}N_4O_8S$: 621.29526, found: 621.29429; HPLC: t_R = 8.58 min (98.9% purity).

4.1.35 (S)-N1-((S)-1-(((S)-1-(furan-2-yl)-4-methyl-1-oxopentan-2-yl)amino)-3-methoxy-1-oxopropan-2-yl)-N4-isopentyl-2-(4-methylphenylsulfonamido)succinamide (11n):

Following the same procedure as described for the synthesis of 11a except for starting from **10a** and **8b**, **11n** was obtained in 81% yield as a white solid; mp: 194-195□; ^{1}H NMR (400 MHz, DMSO-d_6): δ = 0.81 (d, *J* = 6.6 Hz, 6H, CH_3), 0.88 (d, *J* = 6.1 Hz, 6H, CH_3), 1.19-1.24 (m, 2H, CH), 1.41-1.54 (m, 2H, CH_2), 1.61-1.69 (m, 2H, CH_2), 2.22-2.50 (m, 2H, CH_2), 2.37 (s, 3H, CH_3), 2.96 (dd, *J* = 6.6, 13.6 Hz, 2H, CH_2), 3.18 (s, 3H, OCH_3), 3.28 (dd, *J* = 4.1, 9.7 Hz, 1H, CH_2), 3.47 (dd, *J* = 5.5, 9.7 Hz, 1H, CH_2), 4.16-4.18 (m, 2H, CH), 4.86-4.91 (m, 1H, CH), 6.69 (d, *J* = 1.9 Hz, 1H, F-4), 7.33 (d, *J* = 8.0 Hz, 2H, Ph), 7.43 (d, *J* = 3.5 Hz, 1H, F-3), 7.66 (d, *J* = 8.0 Hz, 2H, Ph), 7.85 (t, *J* = 5.1, 10.4 Hz, 1H, NH), 7.99 (s, 2H, NH, F-5), 8.18 (d, *J* = 8.0 Hz, 1H, NH), 8.33 ppm (d, *J* = 7.3 Hz, 1H, NH); ^{13}C NMR (100 MHz, DMSO-d_6): δ = 21.4, 21.8, 22.8, 23.5, 24.7, 25.7, 37.3, 38.2, 39.0, 53.1, 53.3, 53.6, 58.8, 72.0, 112.9, 119.4, 127.0, 129.8, 138.8, 142.8, 148.4, 150.6, 169.2, 169.8, 170.6, 187.5 ppm; HRMS (ESI) *m/z* $[M+H]^+$ calcd for $C_{30}H_{45}N_4O_8S$: 621.29526, found: 621.29436; HPLC: t_R = 8.68 min (99.8% purity).

4.1.36 (S)-N1-((S)-1-(((S)-1-(furan-2-yl)-4-methyl-1-oxopentan-2-yl)amino)-3-methoxy-1-oxopropan-2-yl)-N4-isobutyl-2-(4-methylphenylsulfonamido)succinamide (11o):

Following the same procedure as described for the synthesis of **11a** except for starting from **10b** and **8b**, **11o** was obtained in 75% yield as a white solid; mp: 194-195□; ^{1}H NMR (400 MHz, DMSO-d_6): δ = 0.78 (dd,*J* = 3.4, 6.5 Hz, 6H, CH_3), 0.88 (d,*J* = 4.6 Hz, 6H, CH_3), 1.41-1.48 (m, 1H, CH), 1.56-1.69 (m, 3H, CH_2, CH), 2.28 (dd, *J* = 5.9, 15.1 Hz, 1H, CH_2), 2.37 (s, 3H, CH_3), 2.78 (t, *J* = 6.2 Hz, 2H, CH_2), 3.18 (s, 3H, OCH_3), 3.26-3.33 (m, 2H, CH_2), 3.43-3.48 (m, 1H, CH_2), 4.14-4.22 (m,2H, CH), 4.85-4.92 (m, 1H, CH), 6.69 (dd, *J* = 1.5, 3.4 Hz, 1H, F-4), 7.33 (d, *J* = 8.0Hz, 2H, Ph), 7.43 (d, *J* = 3.5 Hz, 1H, F-3), 7.65 (d, *J* = 8.1 Hz, 1H, Ph), 7.87 (t, *J* = 5.5 Hz, 1H, Ph), 7.95-8.00 (m, 2H, F-5, NH), 8.15 (d, *J* = 7.9 Hz, 1H, NH), 8.33 ppm (d, *J* = 7.4 Hz, 1H, NH); ^{13}C NMR (100 MHz, DMSO-d_6): δ = 20.6, 21.4, 21.9, 23.4, 24.7, 28.3, 39.0, 46.6, 53.1,

53.4, 53.6, 58.7, 72.0, 112.9, 119.4, 127.1, 129.8, 138.8, 142.9, 148.4, 150.7, 169.3, 169.8, 170.6, 187.5 ppm; HRMS (ESI) *m/z* $[M+H]^+$ calcd for $C_{29}H_{43}N_4O_8S$: 607.27961, found: 607.27840; HPLC: t_R = 9.87 min (99.9% purity).

4.2 Biological evaluation

4.2.1 *In vitro* 20S proteasome inhibition assay

The 20S proteasome activity assay kit was purchased from Promega Inc (Cat. # G8531), which consists of three homogeneous bioluminescent assays that measure the three proteolytic activities separately. Human constitutive 20S proteasome was bought from Boston Biochem, USA. The compounds were dissolved in DMSO, serially diluted in 10 mM HEPES (pH 7.6) buffer and combined with 1 μg/mL proteasome, with the final solvent concentration kept constant at 1% (v/v). After incubation for 2 hours at 25 □, individual luminescence substrate was dispensed, and luminescence signals were recorded 10 min on Flex Station 3 multi-mode microplate reader (Molecular Devices) after luminescence substrate Suc-LLVY-Glo™ (for CT-L) or Z-LRR-Glo™ (for T-L) or Z-nLPnLD-Glo™ (for C-L) reagents addition. An inhibition rate was calculated and the IC_{50} value was generated by GraphPad Prism 4.0 software.

4.2.2 SPR analysis

Inhibitors were dissolved in DMSO (10 mM) and then diluted 20-fold in DMSO to achieve a 0.5 mM final stock solution. The above stock solutions were diluted 20-fold in PBS-P buffer (10 mM phosphate buffer with 2.7 mM KCl and 137 mM NaCl, 0.05% surfactant P20, pH 7.4), and the obtained 25 μM solutions were then serially diluted 2-fold in running buffer (10 mM phosphate buffer with 2.7 mM KCl and 137 mM NaCl, 0.05% surfactant P20, 5% DMSO, pH 7.4) to obtain the final 5% (v/v) DMSO concentration series from 25 μM to 1.56 μM and transferred to a 96-well plate. The SPR experiment was conducted on the Biacore T200 system (GE Healthcare, Uppsala, Sweden) at 25 °C. Human 20S proteasome (Boston Biochem, USA) was immobilized on a CM5 chip using an amine coupling kit (GE Healthcare, Buckinghamshire, UK). Final protein immobilized levels were typically ~15,000 RU. Subsequently, inhibitors of various concentrations were injected individually as analytes at a flow rate of 30 μL/min with both association time and dissociation time of 60 s. Chip platforms were washed with running buffer and 50% DMSO. Data were treated using Biacore T200 evaluation software provided by the manufacturer.

Non-specific binding to surface of the chip without proteasome was recorded in parallel and the non-specific signal was subtracted from the sample response with immobilized 20S proteasome to correct for systematic noise and baseline drift. Data were solvent corrected, and the response from the blank injections was used to double reference the binding data. The data were normalized by molecular weight, and rate constants k_{on} and k_{off} values were obtained using the Biacore evaluation software (T200 version 1.0) by curve fitting using a 1:1binding model fit.

4.2.3 LC-MS/MS assay

4.2.3.1 Protein digestion, peptide purification

The purified human 20S proteasome (4 nM) and inhibitors (10 μM) solutions were incubated (500 μL total volume) at room temperature for 2 h. After incubation, 125 μL of acetonitrile was added to quench the reaction and denature the protein. Trypsin was added with an enzyme-to-substrate ratio of 1:50. The digestion was carried out overnight at 37 °C. The digest was concentrated by vacuum centrifugation, and the peptides were desalted using C18 reversed phase pipet tips. An aliquot (50%) of the total digest was injected into the mass spectrometer.

4.2.3.2 LC-MS/MS analysis

For LC-MS/MS analysis, the samples were vacumm-centrifuged to dryness, and reconstituted in 0.2% formic acid, loaded onto a 100μm x 2 cm pre-column and separated on a 75μm × 15 cm capillary column with laser-pulled sprayer. Both columns were packed in-house with 4 μm C18 bulk material (InnosepBio, P. R. China). An Easy nLC 1000 system (Thermo Scientific, USA) was used to deliver the following HPLC gradient: 5-35% B in 75 min, 35-75% B in 4 min, then held at 75% B for 10 min (A = 0.1% formic acid in water, B = 0.1% formic acid in acetonitrile). The eluted peptides were sprayed into a Q Exactive mass spectrometer (Thermo Scientific, USA) equipped with a nano-ESI source. The mass spectrometer was operated in data-dependent mode with a full MS scan in FT mode at a resolution of 70000 followed by HCD (High-energy Collisional Dissociation) MS/MS scans on the top 20 abundant ions in the initial MS scan.

4.2.3.3 Database searching and data analysis

The raw data files were converted to mascot generic format (".mgf") using MS Convert before submitted for database search. Mascot (version 2.3.02) carried out all database search with the following parameters: Carbamidomethyl (Cys) as fixed modification, Oxidation (Met)

as variable modification and potential modifications on threonine (Thr +620.287985 for compound **11m**, and Thr +719.425799 for α′, β′-epoxyketones modification by Carfilzomib); +/- 10 ppm for peptide pass tolerance and +/- 0.02 Da for fragment mass tolerance; max missed cleavages 2.

4.2.4 Reversibility assay

For each reversibility assay, 8 μg/mL 20S proteasome was pre-incubated with each inhibitor at 25 °C for 2 h. For standard assay, pre-incubated lasted for another 4h, and then luminescence substrate Suc-LLVY-Glo™ was added. After incubation at 25 °C for 10 min, the luminescence signals were recorded. For wash-out assay reaction, each pre-incubated reaction mixture was loaded onto Amicon®Ultra-0.5 centrifugal filter devices (100 kDa molecular-weight cut off) and washed five times with the assay buffer by centrifuging at14,000g for 5 min to eliminate excess inhibitor. The proteasome in assay buffer were recovered to the plate by placing the Amicon® Ultra filter device upside down in a clean microcentrifuge tube and spinning for 2 minutes at 1,000 × g. After incubation at 25 °C for another 4 h, luminescence substrate Suc-LLVY-Glo™ was added and the luminescence signals were measured after10 minutes.

4.2.5 Cellular assay

4.2.5.1 Cell Culture and Cytotoxicity Assays

Malignant melanoma (A375), gastriccarcinoma (BGC-823), cervical carcinoma (Hela), colorectal adenocarcinoma (HT-29), lung cancer (A549), prostate cancer (PC3M1E8), colorectal carcinoma (HCT-116) and human embryonic kidney cells (HEK293) were cultured in their respective media supplemented with 10% fetal bovine serum (FBS). The cytotoxicity of inhibitors were measured using Cell Titer-Glo® Luminescent Cell Viability Assay (Promega Inc). The cancer cells growing in log phase were plated at 1000 cells per well. After 18-24 hours, media including the test compounds at corresponding concentrations were added to each well. After 72 hours incubation, an equal volume of Cell Titer-Glo reagent was added, and luminescence was monitored over time with the plates held at 37□. The resulting signals were quantified using a Multimode Microplate Reader Varioskan Flash (Thermo Scientific, USA). The curve-fitting software package Sigma Plot 10.0 was used to generate dose-response curves from which IC_{50} values were determined for active compounds.

4.2.5.2 Cell cycle analysis

HCT-116 cells were planted in 10 cm dish ($2*10^6$cells/dish) and grown in RPMI 1640 containing 10 % fetal bovine serum, 100 U/mL penicillin and 100 μg/mL streptomycin. Cells were treated with either **11c**, **11m**, **11o**, MG132 or vehicle (0.1 % DMSO) for 24 h at 5% CO_2, 37 □. The cells were harvested and washed in cold PBS. Cold 70 % ethanol were added dropwise to the pellets while vortexing. Fixed cells were then kept at -20 □ overnight. Cells were centrifuged for 10 min and washed with 3 mL cold PBS two times. The resulted cell pellets were then resuspended in 500 μL staining solution (0.2 mg/mL RNAse A, 0.03mg/mL propidium iodide, 0.1 % Triton-X 100 in PBS) and for 20 minutes at 37 °C. Samples were then sieved with 400 mesh cell sieve and analyzed on a Beckman CytoFLEX flowcytometry. Histograms were generated and cell cycle analysis was performed using ModFit LT 5.0software (Verity Software House).

4.2.6 *In vivo* studies

Male Sprague-Dawley rats or BALB/c mice were purchased from Vital River Laboratory Animal Technology Inc. (Beijing, China). All animal experiments were approved by the Committee of Peking University on Ethics of Animal Experiments and were conducted in accordance with the Guidelines for Animal Experiments, Peking University Health Science Center.

4.2.6.1 Pharmacokinetics assessment of 11m

Prior to pharmacokinetic study, **11m** was formulated in 8 % ethanol, 2 % Tween 80 and 90 % sterile water. Three adult male Sprague-Dawley rats were used in each group. The animals were fasted for 12 hours before experiment, and then they were given a single dose of **11m** by intravenous injection at 5 mg/kg. Capillary tubes were inserted into the inner canthus and rotated towards the eye ground to open the venous plexus of the rats to draw blood samples into tubes containing sodium heparin. Blood samples were collected at 5 min, 15 min, 30 min, 1h, 2 h, 4 h, 8 h, 24 h, 32 h and 48 h post dose and centrifuged immediately to separate the plasma. The above samples were stored at -20 □ for 2 h and then transferred to -80 □ afterwards until analysis. The plasma **11m** concentrations were measured using **11o** as an internal standard on a LC-MS/MS system (ACQUITY UPLC H-Class – TQD, Waters). First-order compartment model were fitted using the software WinNonlin Enterprise version 4.1 (Pharsight Co., Mountain View, CA).

4.2.6.2 *In Vivo* anti-toumor activity

Six-week-old male BALB/c athymic nude mice were housed under specific pathogen-free conditions for one week before experiment. The xenograft models were developed as described by Milacic et al. [31]. Briefly, mice were implanted subcutaneously with HCT-116 human colon cancer cells (1×10^7 tumor cells/0.1 ml of serum-free RPMI 1640 medium/animal) into the right flanks. After about ten days, the tumors reached a measured volume (~300 mm^3). Mice were randomized into 3 groups (n=3/group). Treatment group with **11m** (in 8 % ethanol, 2 % Tween 80 and 90 % sterile water) was given 10 mg/kg (i.v., twice a week, D1/D4) via tail vein. The positive control group was treated with carfilzomib (in 10% (w/v) sulfobutylether-β-cyclodextrin and 10 mmol/L sodium citrate (pH 3.5)) 5 mg/kg (i.v., twice a week, D1/D4) via tail vein. The vehicle group received the same volume of 8 % ethanol, 2 % Tween 80 and 90 % sterile water. Tumor volumes and the weight of the animals were estimated twice weekly during the experiment. The tumor volumes were measured with Vernier calipers and calculated by the following formula: (length × $(width)^2$)/2.

4.3 Docking study

The 20S proteasome crystal structure (PDB ID: 4NO8) was used due to its structural similarity between its co-crystallized ligand, a tripeptide with a ketoamide warhead, and our furylketone tripeptides. As its original crystallized ligand 6 bound to β5 (cyan) and β6 (white) active sites, we selected chain K and L for further optimization via the Discovery Studio 2.5 software. The 3D model of compound **11m** was built using the 'prepare ligands' protocol of Discovery Studio with modified CHARMm force field applied to give the energy-minimized conformation. Docking simulation was performed via GOLD 3.0.1. The binding site was defined by selecting atoms within 10 Å of ligand 6 from its crystal pose with the cavity detection mode turned on. The default parameters were used, and then the GA (genetic algorithm) Calculations were performed for 100 times. In post docking analysis, cartoon plots were rendered in PyMOL.

Acknowledgment.

This work was generously supported by the National Natural Science Foundation of China (81872731, 21977006, 21807006). The authors also appreciate Dr. Hao Liang from the College of Chemistry and Molecular Engineering, Peking University for his kind technical help on computational simulations.

Present address of the author

§Dr. Qi Sun is now working at BNLMS, State Key Laboratory for Structural Chemistry of Unstable and Stable Species, College of Chemistry and Molecular Engineering, Peking University, Beijing, 100871, China

Supporting Information Available:

Supplementary data related to this article can be found at the online version.

References

[1] Lindquist, S. L.; Kelly, J. W., Chemical and biological approaches for adapting proteostasis to ameliorate protein misfolding and aggregation diseases: progress and prognosis. *Cold Spring Harb Perspect Biol* **2011,** *3*, a004507.

[2] Ciechanover, A., The ubiquitin-proteasome pathway: on protein death and cell life. *Embo Journal* **1998,** *17*, 7151-7160.

[3] Voges, D.; Zwickl, P.; Baumeister, W., The 26S proteasome: A molecular machine designed for controlled proteolysis. *Annu. Rev. Biochem.* **1999,** *68*, 1015-1068.

[4] Groll, M.; Ditzel, L.; Lowe, J.; Stock, D.; Bochtler, M.; Bartunik, H. D.; Huber, R., Structure of 20S proteasome from yeast at 2.4 angstrom resolution. *Nature* **1997,** *386*, 463-471.

[5] Kopp, F.; Hendil, K. B.; Dahlmann, B.; Kristensen, P.; Sobek, A.; Uerkvitz, W., Subunit arrangement in the human 20S proteasome. *Proc. Natl. Acad. Sci. U. S. A.* **1997,** *94*, 2939-2944.

[6] Zwickl, P.; Kleinz, J.; Baumeister, W., Critical elements in proteasome assembly. *Nat. Struct. Biol.* **1994,** *1*, 765-770.

[7] Seemuller, E.; Lupas, A.; Stock, D.; Lowe, J.; Huber, R.; Baumeister, W., Proteasome from thermoplasm-acidophilum - a threonine protease. *Science* **1995,** *268*, 579-582.

[8] Tomko, R. J., Jr.; Hochstrasser, M., Molecular architecture and assembly of the eukaryotic proteasome. *Annu. Rev. Biochem.* **2013,** *82*, 415-45.

[9] Chen, P.; Hochstrasser, M., Autocatalytic subunit processing couples active site formation in the 20S proteasome to completion of assembly. *Cell* **1996,** *86*, 961-972.

[10] An, B.; Goldfarb, R. H.; Siman, R.; Dou, Q. P., Novel dipeptidyl proteasome inhibitors overcome Bcl-2 protective function and selectively accumulate the cyclin-dependent kinase inhibitor p27 and induce apoptosis in transformed, but not normal, human fibroblasts. *Cell Death*

Differ. **1998,** *5*, 1062-1075.

[11] Lopes, U. G.; Erhardt, P.; Yao, R. J.; Cooper, G. M., p53-dependent induction of apoptosis by proteasome inhibitors. *J. Biol. Chem.* **1997,** *272*, 12893-12896.

[12] Dou, Q. P.; Li, B. Y., Proteasome inhibitors as potential novel anticancer agents. *Drug Resist. Update* **1999,** *2*, 215-223.

[13] Kisselev, A. F.; Goldberg, A. L., Proteasome inhibitors: from research tools to drug candidates. *Chemistry & Biology* **2001,** *8*, 739-758.

[14] Gandolfi, S.; Laubach, J. P.; Hideshima, T.; Chauhan, D.; Anderson, K. C.; Richardson, P. G., The proteasome and proteasome inhibitors in multiple myeloma. *Cancer Metastasis Rev* **2017,** *36*, 561-584.

[15] Sun, Q.; Xu, B.; Niu, Y.; Xu, F.; Liang, L.; Wang, C.; Yu, J.; Yan, G.; Wang, W.; Jin, H.; Xu, P., Synthesis, bioactivity, docking and molecular dynamics studies of furan-based peptides as 20S proteasome inhibitors. *ChemMedChem* **2015,** *10*, 498-510.

[16] Beck, P.; Dubiella, C.; Groll, M., Covalent and non-covalent reversible proteasome inhibition. *Biol Chem* **2012,** *393*, 1101-20.

[17] Fu, Y.; Xu, B.; Zou, X.; Ma, C.; Yang, X.; Mou, K.; Fu, G.; Lv, Y.; Xu, P. Design and synthesis of a novel class of furan-based molecules as potential 20S proteasome inhibitors. *Bioorg. Med. Chem. Lett.* **2007**, *17*, 1102-1106.

[18] Rydzewski, R. M.; Burrill, L.; Mendonca, R.; Palmer, J. T.; Rice, M.; Tahilramani, R.; Bass, K. E.; Leung, L.; Gjerstad, E.; Janc, J. W.; Pan, L. Optimization of subsite binding to the β5 subunit of the human 20S proteasome using vinyl sulfones and 2-keto-1,3,4-oxadiazoles: syntheses and cellular properties of potent, selective proteasome inhibitors. *J. Med. Chem.* **2006**, *49*, 2953-2968.

[19] Parlati, F.; Lee, S. J.; Aujay, M.; Suzuki, E.; Levitsky, K.; Lorens, J. B.; Micklem, D. R.; Ruurs, P.; Sylvain, C.; Lu, Y.; Shenk, K. D.; Bennett, M. K. Carfilzomib can induce tumor cell death through selective inhibition of the chymotrypsin-like activity of the proteasome. *Blood* **2009**, *114*, 3439−3447.

[20] Demo, S. D.; Kirk, C. J.; Aujay, M. A.; Buchholz, T. J.; Dajee, M.; Ho, M. N.; Jiang, J.; Laidig, G. J.; Lewis, E. R.; Parlati, F.; Shenk, K. D.; Smyth, M. S.; Sun, C. M.; Vallone, M. K.; Woo, T. M.; Molineaux, C. J.; Bennett, M. K. Antitumor activity of PR-171, a novel irreversible inhibitor of the proteasome. *Cancer Res.* **2007**, *67*, 6383–6391.

[21] Ozcan, S.; Kazi, A.; Marsilio, F.; Fang, B.; Guida, W. C.; Koomen, J.; Lawrence, H. R.; Sebti, S. M. Oxadiazole-isopropylamides as Potent and Noncovalent Proteasome Inhibitors. *J. Med. Chem.* **2013**, *56*, 3783−3805.

[22] Kazi, A.; Ozcan, S.; Tecleab, A.; Sun, Y.; Lawrence, H. R.; Sebti, S. M. Discovery of PI-1840, a Novel Noncovalent and Rapidly Reversible Proteasome Inhibitor with Anti-tumor Activity, *J. Biol. Chem.* **2014**, *289*, 11906-11915.

[23] Lansdell, T. A.; Hurchla, M. A.; Xiang, J.; Hovde, S.; Weilbaecher, K. N.; Henry, R. W.; Tepe, J. J. Noncompetitive Modulation of the Proteasome by Imidazoline Scaffolds Overcomes Bortezomib Resistance and Delays MM Tumor Growth in Vivo. *ACS Chem. Biol.* **2013**, *8*, 578-587.

[24] Kupperman, E.; Lee, E. C.; Cao, Y.; Bannerman, B.; Fitzgerald, M.; Berger, A.; Yu, J.; Yang, Y.; Hales, P.; Bruzzese, F.; Liu, J.; Blank, J.; Garcia, K.; Tsu, C.; Dick, L.; Fleming, P.; Yu, L.; Manfredi, M.; Rolfe, M.; Bolen, J. Evaluation of the Proteasome Inhibitor MLN9708 in Preclinical Models of Human Cancer. *Cancer Res.* **2010**, *70*, 1970-1980.

[25] Bedford, L.; Lowe, J.; Dick, L. R.; Mayer, R. J.; Brownell, J. E. Ubiquitin-like protein conjugation and the ubiquitin–proteasome system as drug targets. *Nature Rev. Drug Discov.*, **2011**, 10, 29-46.

[26] Stein, M. L.; Cui, H.; Beck, P.; Dubiella, C.; Voss, C.; Krü ger, A.; Schmidt, B.; Groll, M. Systematic comparison of peptidic proteasome inhibitors highlights the α-ketoamide electrophile as an auspicious reversible lead motif. *Angew. Chem. Int. Ed. Engl.* **2014**, *53*, 1679-83.

[27] Hartmann□Petersen, R.; Gordon, C. Quantifying protein-protein interactions in the ubiquitin pathway by surface plasmon resonance. *Meth. Enzymol.* **2005**, *399*, 164-177.

[28] Gorodkiewicz, E.; Ostrowska, H.; Sankiewicz, A. SPR imaging biosensor for the 20S proteasome: sensor development and application to measurement of proteasomes in human blood plasma. *Microchim Acta* **2011**, *175*, 177-184.

[29] Yang, J.; Wang, Z.; Fang, Y.; Jiang, J.; Zhao, F.; Wong, H.; Bennett, M. K.; Molineaux, C. J.; Kirk, C. J. Pharmacokinetics, Pharmacodynamics, Metabolism, Distribution, and Excretion of Carfilzomib in Rats. *Drug Metab. Dispos.* **2011**, *39*, 1873-1882.

[30] Probst, R. J.; Lim, J. M.; Bird, D. N.; Pole, G. L.; Sato, A. K.; Claybaugh, J. R. Gender differences in the blood volume of conscious Sprague-Dawley rats. *J. Am. Assoc. Lab Anim. Sci.* **2006**, *45*, 49-52.

[31] Milacic, V.; Banerjee, S.; Landis-Piwowar, K. R.; Sarkar, F. H.; Majumdar, A. P. N.; Dou, Q. P. Curcumin Inhibits the Proteasome Activity in Human Colon Cancer Cells In vitro and In vivo. *Cancer Res*. **2008**, 68, 7283-7292.

Highlights

- A series of tripeptidic proteasome inhibitors with furylketone as C-terminus were found acting selectively against the β5 subunit.
- The optimized Compd. **11m** shows potency comparable to MG132 at both enzymatic and cellular levels.
- **11m** inhibits 20S proteasome reversibly, and binds with it in "rapid loading and slowly dissociation" mode.
- The pharmacokinetic profiles of **11m** in rats suggested a broader distribution *in vivo* than carfilzomib.
- **11m** was able to inhibit tumor growth in xenograft model with potency not surpassing carfilzomib.

Declaration of interests

☒ The authors declare that they have no known competing financial interests or personal relationships that could have appeared to influence the work reported in this paper.

☐The authors declare the following financial interests/personal relationships which may be considered as potential competing interests: